View metadata, citation and similar papers at core.ac.uk

brought to you by CORE

provided by Universidade do Minho: RepositoriUM

Shear Strengthening of RC beams by means of NSM CFRP strips: a proposal for modeling debonding

Vincenzo Bianco, Joaquim Barros and Giorgio Monti

Report 07-DEC/E-29

Date: September of 2007
N. of pages: 48
Keywords: CFRP, NSM, Reinforced Concrete, Debonding

Universidade do Minho

Escola de Engenharia
Departamento de Engenharia Civil

Sapienza University of Rome

Department of Structural Engineering and Geotechnics

Table of Contents

Notation

A_c = area of the concrete prism cross section

A_f = area of the strip's cross section

A^{sf} = constant entering the expression to determine the amount of transfer length undergoing the softening friction bond phase

A^{e} = constant entering the expression to determine the amount of transfer length undergoing the elastic bond phase

A^{s} = constant entering the expression to determine the determine the amount of transfer length undergoing the softening bond phase

B^{sf} = constant entering the expression to determine the softening friction transfer length

B^{e} = constant entering the expression to determine the elastic transfer length

B^{s} = constant entering the expression to determine the softening transfer length

C_1^{fs} = first integration constant for the free slipping phase

C_2^{fs} = second integration constant for the free slipping phase

C_1^{e} = first integration constant for the elastic phase

C_2^{e} = second integration constant for the elastic phase

C^{sf} = constant entering the expression to determine the softening friction transfer length

C^{s} = constant entering the expression to determine the softening transfer length

C_1^{s} = first integration constant for the softening phase

C_2^{s} = second integration constant for the softening phase

C_1^{sf} = first integration constant for the softening friction phase

C_2^{sf} = second integration constant for the softening friction phase

E_c = concrete Young's modulus

E_f = strips' CFRP Young's modulus

J_1 = constant present in the governing differential equation with unknown $\delta(x)$

J_2 = constant present in the equation necessary to determine $\sigma_f(x)$

J_3 = constant present in the equation necessary to determine $\tau(x)$

L_{fi} = i-th strip available bond length

$L_{fi}^{c}(t_n;q_n)$ = height of the concrete semi-cone in correspondence of the i-th strip

L_p = effective perimeter of the strip cross section

$L_{Rfi}(t_n;q_n)$ = i-th strip resisting bond length

$L_{tr,i}(L_{Rfi};\delta_{Li})$ = transfer length of the i-th strip for the relevant imposed slip and current value of the resisting transfer length

$L_{tr}(\delta_{Li})$ = total transfer length for an infinite bond length

L_{tr1} = maximum invariant value of transfer length that can be subject to elastic bond phase

L_{tr2} = maximum invariant value of transfer length that can be subject to softening

L_{tr3} = maximum invariant value of transfer length that can be subject to softening friction

$L_{tr}^{fs}(\delta_{Li})$ = amount of a transfer length for an infinite bond length undergoing free slipping

$L_{tr}^{e}(\delta_{Li})$ = amount of a transfer length for an infinite bond length undergoing elastic phase

$L_{tr}^{sf}(\delta_{Li})$ = softening frictional amount of a transfer length for an infinite bond length

$L_{tr}^{s}(\delta_{Li})$ = amount of a transfer length for an infinite bond length undergoing softening

$OXYZ$ = crack plane reference system

$O_i^l X_i^l$ = reference axis along the i-th strip available bond length L_{fi}

V_c = vertex of the i-th concrete semi-cone

$V_{fi}^{cf}(X_i^l)$ = progressive concrete strength along the i-th strip

$V_{fi}^{bd}(L_{Rfi};\delta_{Li};x_i^{tr})$ = progressive value of the force transferred to concrete by the i-th strip

$V_{fi}^{bd}(L_{Rfi};\delta_{Li})$ = actual value of force transferred to concrete by bond in correspondence of the i-th strip

$V^{bd,e}(\delta_{Li})$ = force transferred by bond in the elastic phase for an infinite bond length

$V^{bd,s}(\delta_{Li})$ = force transferred by bond in softening phase for an infinite bond length

$V^{bd,sf}(\delta_{Li})$ = force transferred by bond in the softening friction phase for an infinite bond length

V_1^{db} = value of force transferred by bond along the elastic transfer length L_{tr1}

V_2^{db} = value of force transferred by bond along the softening transfer length L_{tr2}

V_3^{db} = value of force transferred by bond along the softening friction transfer length L_{tr3}

X_{fi} = position of the i-th strip along the CDC

a_c = concrete prismatic specimen thickness

a_f = strip cross section's thickness

b_c = concrete prismatic specimen width

b_f = strip cross section's width

f_{ctm} = concrete average tensile strength

$o^{fs}x^{fs}$ = reference axis along the amount of the infinite strip in free slipping bond phase

$o^{e}x^{e}$ = reference axis along the amount of the infinite strip in elastic bond phase

$o^{s}x^{s}$ = reference axis along the amount of the infinite strip in softening bond phase

$o^{sf}x^{sf}$ = reference axis along the amount of the infinite strip in softening friction bond phase

$o_i^{tr}x_i^{tr}$ = reference axis along the strip's transfer length the loaded end

q_e = iteration in correspondence of which equilibrium is attained

q_n = n-th iteration

t_0 = load step of formation of the critical diagonal crack

t_1 = load step in correspondence of which the critical diagonal crack starts widening

t_n = generic n-th load step

$u_c(x)$ = punctual displacement of the concrete surrounding the strip

$u_f(x)$ = punctual displacement of the strip

x_1^{fs} = first integration point for calculating the slip along free slipping bond

x_2^{fs} = second integration point for calculating the slip along free slipping bond

x_1^{e} = first integration point for calculating the force transferred by elastic bond

x_2^{e} = second integration point for calculating the force transferred by elastic bond

x_1^{s} = first integration point for calculating the force transferred by softening bond

x_2^{s} = second integration point for calculating the force transferred by softening bond

x_1^{sf} = first integration point for calculating the force transferred by softening friction bond

x_2^{sf} = second integration point for calculating the force transferred by softening friction bond

α = angle between the axis and the generatrices of the i-th concrete semi-cone

β = constant entering the governing differential equation for the softening phase

φ = angle necessary to determine the softening-subject amount of transfer length

$\delta(x)$ = slip along the strip's length

δ_1 = slip corresponding to peak of local bond stress-slip relationship

δ_2 = slip corresponding to start of softening-friction in the local bond relationship

δ_3 = slip corresponding to the start of free-slipping in the local bond stress-slip relationship

$\delta_{Fi}(\delta_{Li}; L_{fi})$ = free end slip for the case of a finite bond length

δ_{Fi} = slip at the free extremity of the i-th strip

$\delta_{Li}[\gamma(t_n); X_{fi}]$ = imposed slip at the loaded extremity of the i-th strip

$\delta^{fs}(x^{fs})$ = slip-abscissa relationship along the amount of transfer length in free slipping phase

$\delta^{e}(x^{e})$ = slip-abscissa relationship along the amount of transfer length in elastic phase

$\delta^{s}(x^{s})$ = slip-abscissa relationship along the amount of transfer length in the softening phase

$\delta^{sf}(x^{sf})$ = slip-abscissa relationship along the amount of transfer length in the softening friction

$\gamma(t_n)$ = critical diagonal crack opening angle

$\dot{\gamma}$ = imposed angle increment for the critical diagonal crack

λ = constant entering the governing differential equation for the elastic phase

θ = shear crack inclination angle

$\tau(\delta)$ = local bond stress-slip relationship

$\tau(x)$ = bond stress along the strip's length

τ_0 = adhesive-cohesive initial bond strength

τ_1 = peak stress of the local bond stress-slip relationship

τ_2 = shear strength at the beginning of softening-friction of local bond

$\sigma_f(x)$ = strip's axial stress

$\sigma_c(x)$ = concrete axial stress

1 Introduction

The most recent works devoted at appraising the potentialities of the technique of Near Surface Mounted (NSM) FRP strips for the shear strengthening of Reinforced Concrete (RC) beams (Dias and Barros 2006, De Lorenzis and Rizzo 2006) spotlighted the occurrence of a failure mode consisting of the progressive detachment of the concrete cover from the core of the beam. That eventuality was even more evident in the case of low strength concrete (Dias *et al.* 2007). A successive analytical investigation (Bianco *et al.* 2007a) demonstrated that this occurrence can be ascribed to the semi-conical fracture of concrete surrounding each NSM strip. When the principal tensile stresses transferred to the surrounding concrete exceed its tensile strength, concrete fractures along the surface envelope of the compression isostatics. It was also outlined (Bianco *et al.* 2006, Bianco *et al.* 2007b) that, in order for a modeling strategy to be comprehensive, it is also necessary to envisage that NSM strips might fail by debonding or tensile rupture. In fact, when concrete mechanical properties are high or the interaction between subsequent strips low and for longer bond lengths, failure may be governed by either loss of bond or tensile rupture. The term "debonding" is adopted to designate failure occurring within the adhesive or just a few millimeters inside the surrounding concrete. Bianco *et al.* (2006) also developed an analytical model for predicting the NSM CFRP strips shear strengthening contribution taking into account the above failure modes. In that occasion, the modeling strategy adopted to simulate the concrete fracture failure mode was developed in closed form resulting robust and rational. The strategy adopted to simulate the possibility of debonding, was, however, based on analytical expressions deduced by regression of experimental recordings. That part of the analytical model results not scientifically rigorous and, therefore, susceptible of improvements. Moreover, among the possible failure modes affecting the behavior, at ultimate, of an NSM CFRP strip, a mixed failure mode composed of a shallow semi-cone plus debonding should be also taken into consideration, see Fig. 1.1. The purpose of the present work is to further address the issue of the debonding process deducing closed-form analytical expressions to be implemented in the framework of the already existing analytical model. Furthermore, the above mentioned analytical model also needs to be improved by including kinematic compatibility since it assumes that all of the strips crossing the critical diagonal crack reach their ultimate state simultaneously, which is not properly the case of a system of FRPs bridging a shear crack (Monti and Liotta 2007).

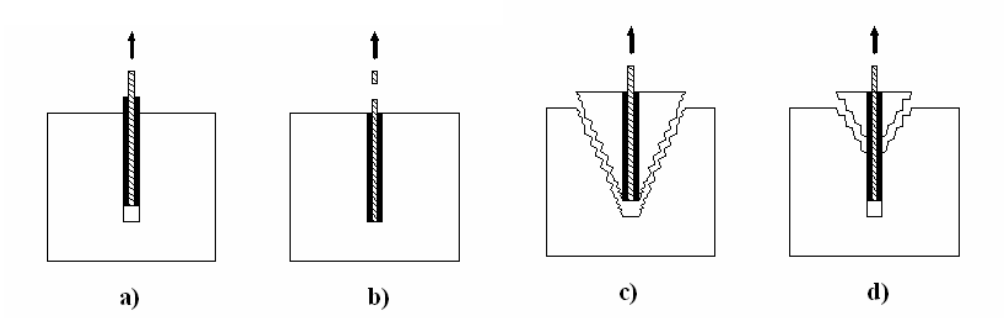

Fig. 1.1 – Possible failure modes affecting an NSM FRP strip: (a) debonding, (b) strip tensile rupture, (c) concrete semi-conical fracture, (d) mixed shallow semi-cone plus debonding.

2 Unified approach for modeling the NSM strips contribution for shear strengthening RC beams

2.1 The algorithm

During the loading process of a RC beam subject to shear, when the concrete average tensile strength f_{ctm} is exceeded at the web intrados, some shear cracks originate therein and successively progress towards the web extrados. Those cracks can be thought of as a single, concentrated, critical diagonal crack (CDC) inclined of an angle θ with respect to the beam longitudinal axis, see Fig. 3.1.

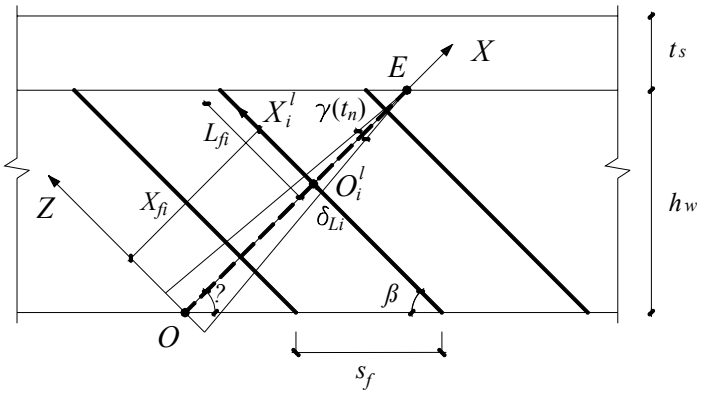

Fig. 3.1 – Lateral view of the strengthened side of the web.

The CDC can be schematized like an inclined plane slicing the web into two portions sawn together by the crossing laminates. It is possible to single out, for each i-the laminate crossing the CDC, the relevant "available bond length" L_{fi}, that is the shorter between the two parts in which the crack divides it. At the load step t_1 the two parts into which the web is divided start to move apart swiveling around the crack end. From that step on, by increasing the applied load, the opening angle of the CDC $\gamma(t_n)$ progressively widens. In that way, the extremities O_i^l of the available bond lengths lying on the CDC start being subjected to an increasing imposed slip $\delta_{Li}[\gamma(t_n), X_{fi}]$ that is function of both the load step t_n, and the position of the laminate along the crack X_{fi}. In correspondence of each constant value of the incremental angle $\gamma(t_n)$, the behavior of the structural system composed of the strips, the adhesive layer and the surrounding concrete is extremely complex. Nonetheless, that behavior can be easily explained by taking into consideration the simplified case of strips orthogonal to the CDC and placed at a large spacing between each other so as to exclude the presence of interaction among them. That particular case lets attention be focused on i-th strip only (Fig. 3.2). The above mentioned behavior can be described by an iterative process aiming at determining, for a given value of $\gamma(t_n)$, the state of equilibrium of the structural system involved. The n-th iteration is indicated by q_n ranging from q_1 (first iteration) to q_e (iteration in correspondence of which equilibrium is attained). Each strip opposes the widening of the crack by anchoring to the surrounding concrete to which it transfers, by bond, the force that originates in its loaded extremity due to the imposed slip.

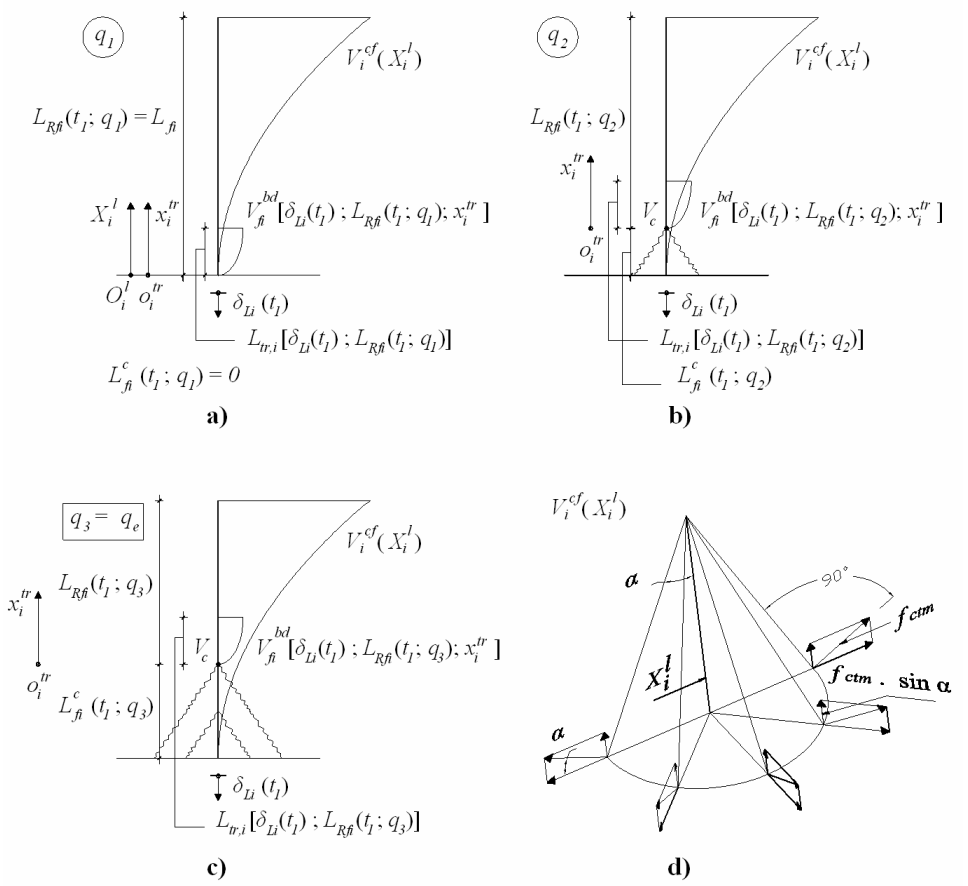

Fig. 3.2 – Formation of the concrete semi-conical fracture surface for the first imposed slip and iterative search for equilibrium: a) bond-transferred force V_{fi}^{bd} exceeding concrete tensile strength V_{fi}^{cf}, b) second iteration and inward movement of the point of application of the imposed slip, c) third iteration and equilibrium attainment, d) concrete fracture strength $V_{fi}^{cf}\left(X_i^l\right)$.

Within each iteration q_n, it is possible to single out, for each i-th strip, the following quantities:

- $L_{Rfi}(t_n; q_n)$ the "resisting bond length" *i.e.* the current amount of L_{fi} that still results embedded in the concrete core of the beam web;
- $L_{fi}^c(t_n; q_n)$ the "concrete semi-cone height" *i.e.* the amount of L_{fi} in correspondence of which the surrounding concrete has fractured along a semi conical surface;
- $L_{tr,i}\left[\delta_{Li}(t_n); L_{Rfi}(t_n; q_n)\right]$ the "transfer length" *i.e.* the amount of L_{Rfi} along which the i-th strip transfers the corresponding force V_{fi}^{bd} to the surrounding concrete;
- $V_{fi}^{bd}\left[\delta_{Li}(t_n); L_{Rfi}(t_n; q_n); x_i^{tr}\right]$ the progressive value of the force transferred by bond to the surrounding concrete along $L_{tr,i}$, where x_i^{tr} represents the reference axis along $L_{tr,i}$.
- $V_{fi}^{bd}\left[\delta_{Li}(t_n); L_{Rfi}(t_n; q_n)\right]$ the actual value of the force transferred by bond to the surrounding concrete along $L_{tr,i}$, given by $V_{fi}^{bd}\left[\delta_{Li}(t_n); L_{Rfi}(t_n; q_n); L_{tr,i}\right]$.

When the i-th strip is subjected to the first imposed end slip $\delta_{Li}(t_1)$, the resulting force $V_{fi}^{bd}\left[\delta_{Li}(t_1);L_{Rfi}(t_1;q_1)\right]$ is transferred to the surrounding concrete by bond along the corresponding transfer length $L_{tr,i}(t_1;q_1)$ that results equal to L_{fi}. The progressive value of that force along the corresponding transfer length, has to result, to assure equilibrium, lower than the concrete strength. The progressive strength offered by concrete $V_{fi}^{cf}\left(X_i^l\right)$ is obtained by spreading the average tensile strength f_{ctm} throughout the resulting semi-conical surface with vertex in X_i^l, integrating and projecting in the laminate direction (Fig. 3.2d), where $O_i^l X_i^l$ is the reference axis along the available bond length of the i-th strip. For the simplified case of absence of interaction between adjacent strips and strips orthogonal to the crack, the progressive value of the concrete tensile strength is given by (Bianco *et al.* 2006): $V_{fi}^{cf}\left(X_i^l\right)=\pi/2\cdot f_{ctm}\cdot tg^2\alpha\cdot\left(X_i^l\right)^2$, where α is the angle between the axis and the generatrices of the semi-conical surface (Fig. 3.2d). If along the transfer length, scanned from the loaded end inward, the progressive value of the force transferred to the surrounding concrete $V_{fi}^{bd}\left(x_i^{tr}\right)$ exceeds the corresponding progressive value of the concrete strength $V_{fi}^{cf}\left(X_i^l\right)$, concrete fractures. A semi-conical shaped macro-crack results, whose vertex V_c is in the innermost point in which it results $V_{fi}^{bd}\left(x_i^{tr}\right)\geq V_{fi}^{cf}\left(X_i^l\right)$. For the example of Fig. 3.2, since equilibrium has not been attained yet, it is necessary to iterate. The force transfer mechanism skips inward to the remaining embedded part of the laminate $L_{Rfi}(t_1;q_2)$ (Fig. 3.2b) and again, if along it the progressive value of the force transferred exceeds the concrete tensile strength, another semi-conical shaped macro crack forms and a further slice detaches from the inner concrete. This process continues until, for the unchanged value of the imposed slip, equilibrium is reached within concrete (Fig. 3.2c). At the successive increments of imposed slip, that process recurs and further semi-conical cracks might occur as spotlighted by Fig. 3.3, in which progressively thicker lines represent the force transferred by bond to concrete along the corresponding transfer length for increasing values of the imposed slip. It can happen that, for a certain value of the imposed slip, after formation of a series of semi-conical shaped concrete slices, the left amount of embedded length fails by debonding (Fig. 3.4). This justifies the possibility of a mixed shallow cone plus debonding failure mode as spotlighted in the case of adhesive anchors (Cook *et al.* 1998). At the same time, and especially for a short bond length, the process of formation of consecutive semi-conical shaped slices of concrete can reach the free end so as, at ultimate, an overall semi-cone of concrete forms, whose height results to be as long as the initial available bond length (Fig. 3.5). It arises that the spacing between successive semi-conical macro cracks also depends on the magnitude of the CDC angle increment rate $\dot{\gamma}$. When equilibrium is attained, each strip contribution is equal to the minimum among the bond transferred force $V_{fi}^{bd}(t_n;q_e)$, the concrete strength $V_{fi}^{cf}(t_n;q_e)$ and the laminate tensile strength V_{fi}^{tr}.

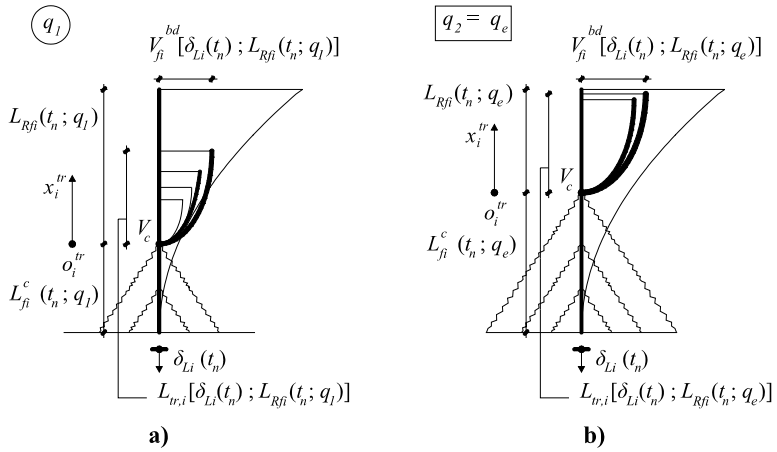

Fig. 3.3 – Formation of successive concrete semi-conical fracture surfaces: a) variation of the force transferred for increasing values of the imposed slip and b) equilibrium configuration.

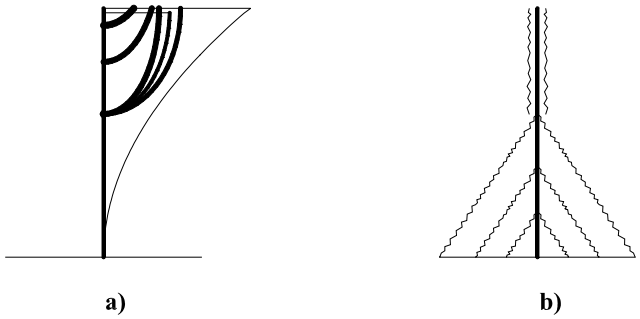

Fig. 3.4 – Mixed shallow semi-cone plus debonding failure mode: a) variation of the force transferred to concrete for increasing values of the imposed slip and b) configuration of the NSM laminate at ultimate.

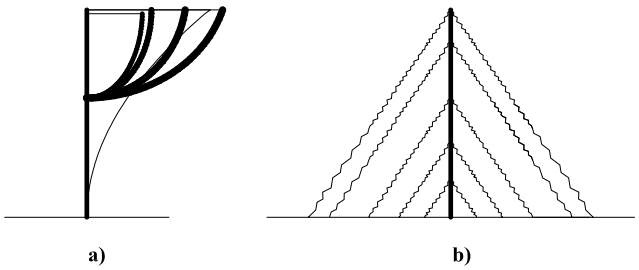

Fig. 3.5 – Concrete semi-conical fracture failure mode: a) variation of the force transferred to concrete for increasing values of the imposed slip and b) configuration of the NSM laminate at ultimate.

In the case in which the simplified hypothesis of large spacing among laminates is abandoned, strips interact with each other and the relevant the semi-conical fracture surfaces overlap (Fig. 3.6). When the interaction between adjacent strips cannot be neglected and when they do not result orthogonal to the crack plane, the calculation of the concrete tensile strength contribution $V_{fi}^{cf}\left(X_i^l;t_n;q_n\right)$ complicates. A closed form algorithm is adopted to calculate that strength as function of the several parameters involved *i.e.*: $V_{fi}^{cf}\left(X_i^l;t_n;q_n\right)=f\left[f_{ctm};\alpha;\theta;\beta;s_f;h_w;b_w;L_j^c\left(t_n;q_n\right)\forall\, j=1,..N_f\right]$ where s_f is the spacing between strips measured along the beam axis, h_w and b_w the height and width of the web and

N_f the number of strips crossing the crack. For the sake of brevity, the details of the aforementioned algorithm are herein omitted but they can be found elsewhere (Bianco *et al.* 2006 and 2007c).

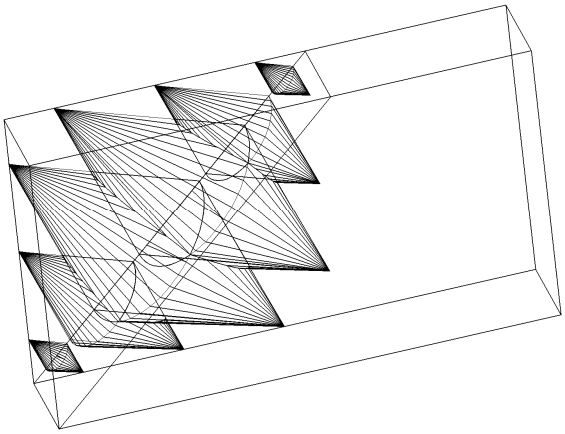

Fig. 3.6 – Interaction between adjacent strips: inside view of the fracture surface resulting from the overlapping of semi-conical fracture surfaces on one side of the web.

2.2 Pure Debonding Model

As stressed above, the modeling strategy adopted to simulate the loss of bond of the NSM strips, in the ambit of the analytical model developed by Bianco *et al.* (2006) to calculate the NSM shear strength contribution to RC beams is susceptible of improvements. The understanding and analytical modeling of debonding affecting the behavior of externally bonded FRPs has reached to date, a high level of accuracy (Monti *et al.* 2003, Yuan *et al.* 2004, Mohammed Ali *et al.* 2006). As regards more specifically the case of NSM strips it arises, from the most recent works (Sena-Cruz 2004, Sena-Cruz and Barros 2004, Borchert and Zilch 2007), that debonding is more complicated, mainly because of the higher number of parameters it depends on. Moreover, several aspects still need to be clarified. In the present work, the main purpose to improve a shear-devoted analytical predictive model already existing, prompted the authors to further address some of those aspects and to provide a new interpretation of the phenomenon. By analyzing the most recent specialized publications, regarding the newest findings in terms of employment of high performance adhesives in technical applications (see, for instance: Sekulic and Curnier 2006, Zhai *et al.* 2007), it arises that, due to the relevant novelty of those materials, a lot of aspects still need to be clarified, even from a micro-structural and chemical standpoint. In that scenario, a new interpretation of the phenomenon of loss of bond for an NSM CFRP strip is provided by putting forward some hypotheses that should be further confirmed, *a posteriori*, also by means of more specialized contributions.

3 Governing Equations

The equations reported hereafter, are derived referring to a typical push-pull test of a CFRP strip near surface mounted on a prism of concrete. The width and thickness of the strip are denoted by b_f and a_f respectively, those of the concrete prism by b_c and a_c respectively. The Young's modulus of the strip and concrete is E_f and E_c respectively. Based on equilibrium considerations, the following fundamental equations can be found:

$$\frac{d\sigma_f(x)}{dx} - \tau(x) \cdot \frac{L_p}{A_f} = 0 \tag{3.1}$$

$$\sigma_f(x) \cdot A_f + \sigma_c(x) \cdot A_c = 0 \tag{3.2}$$

where $\tau(x)$ is the shear stress acting on the surface of the strip, $\sigma_f(x)$ is the axial stress in the strip, $\sigma_c(x)$ is the axial stress in the concrete prism, A_f ($a_f \cdot b_f$) and A_c ($a_c \cdot b_c$) are the area of the cross section of the strip and concrete prism, respectively, and L_p is the effective bond perimeter of the cross section *i.e.*:

$$L_p = 2 \cdot b_f + a_f \tag{3.3}$$

The constitutive equations for the adhesive layer and the two adhering materials can be written as:

$$\tau = \tau(\delta) \tag{3.4}$$

$$\sigma_f = E_f \cdot \frac{du_f}{dx} \tag{3.5}$$

$$\sigma_c = E_c \cdot \frac{du_c}{dx} \tag{3.6}$$

The interfacial slip δ is defined as the punctual relative displacement between the two adhering materials, that is:

$$\delta(x) = u_f(x) - u_c(x) \tag{3.7}$$

From Eq. 3.2 it is:

$$\sigma_f = -\cdot \frac{\sigma_c \cdot A_c}{A_f} \rightarrow \frac{d\sigma_f}{dx} = -\frac{A_c}{A_f} \cdot \frac{d\sigma_c}{dx} \tag{3.8}$$

and, introducing Eq. 3.6 it becomes:

$$\frac{d\sigma_f}{dx} = -\frac{A_c}{A_f} \cdot E_c \cdot \frac{d}{dx}\left(\frac{du_c}{dx}\right) \tag{3.9}$$

From Eq. 3.7 it is:

$$u_c(x) = u_f(x) - \delta(x) \tag{3.10}$$

Introducing Eq. 3.10 into Eq. 3.9, it becomes:

$$\frac{d\sigma_f}{dx} = -\frac{A_c}{A_f} \cdot E_c \cdot \frac{d}{dx}\left(\frac{du_f}{dx} - \frac{d\delta}{dx}\right) \tag{3.11}$$

and, since from Eq. 3.5 it is:

$$\frac{du_f}{dx} = \frac{\sigma_f}{E_f} \tag{3.12}$$

Then Eq. 3.11 becomes:

$$\frac{d\sigma_f}{dx} = -\frac{A_c}{A_f} \cdot E_c \cdot \frac{d}{dx}\left(\frac{\sigma_f}{E_f} - \frac{d\delta}{dx}\right) \tag{3.13}$$

and solving it with respect to $d\sigma_f / dx$ we obtain:

$$\frac{d\sigma_f}{dx} = \frac{A_c \cdot E_c}{A_f} \cdot \frac{1}{\left[1 + \frac{A_c \cdot E_c}{A_f \cdot E_f}\right]} \cdot \frac{d^2\delta}{dx^2} \tag{3.14}$$

Introducing Eq. 3.14 into Eq. 3.1 it results:

$$\frac{d^2\delta}{dx^2} - \tau(x) \cdot \frac{L_p}{A_f} \cdot \left(\frac{1}{E_f} + \frac{A_f}{A_c \cdot E_c}\right) = 0 \tag{3.15}$$

That can be rewritten as follows:

$$\frac{d^2\delta}{dx^2} - \tau[\delta(x)] \cdot J_1 = 0 \tag{3.16}$$

with:

$$J_1 = \frac{L_p}{A_f} \cdot \left(\frac{1}{E_f} + \frac{A_f}{A_c \cdot E_c}\right) \tag{3.17}$$

Eq. 3.16 is the governing differential equation that can be solved for whatever boundary conditions once the local bond stress-slip relationship is reliably known.

Once the relationship $\delta(x)$ has been determined, the expressions for the stress in the strip and the tangential stress along this latter can be deduced as hereafter reported.

Introducing Eq. 3.7 into Eq. 3.5, we obtain:

$$\sigma_f = E_f \cdot \frac{d}{dx}[\delta(x) + u_c(x)] = E_f \cdot \left[\frac{d\delta}{dx} + \frac{du_c}{dx}\right] \tag{3.18}$$

and, introducing Eq. 3.6, it becomes:

$$\sigma_f = E_f \cdot \left[\frac{d\delta}{dx} + \frac{\sigma_c}{E_c}\right] \tag{3.19}$$

but since from Eq. 3.2 it is:

$$\sigma_c = -\cdot \frac{\sigma_f \cdot A_f}{A_c} \tag{3.20}$$

former Eq. 3.19 becomes:

$$\sigma_f \cdot \left[1 + \frac{E_f \cdot A_f}{E_c \cdot A_c}\right] = E_f \cdot \frac{d\delta}{dx} \tag{3.21}$$

that can be rewritten like:

$$\sigma_f(x) = J_2 \cdot \frac{d\delta}{dx} \tag{3.22}$$

with:

$$J_2 = \frac{E_f \cdot E_c \cdot A_c}{E_c \cdot A_c + E_f \cdot A_f} \tag{3.23}$$

Likewise, from Eq. 3.1 it is:

$$\tau(x) \cdot \frac{L_p}{A_f} = \frac{d\sigma_f(x)}{dx} \tag{3.24}$$

but, from previous Eq. 3.21, it is:

$$\frac{d\sigma_f}{dx} = \frac{E_f \cdot E_c \cdot A_c}{E_c \cdot A_c + E_f \cdot A_f} \cdot \frac{d^2\delta}{dx^2} \tag{3.25}$$

thus, Eq. 3.24 becomes:

$$\tau(x) = \frac{A_f}{L_p} \cdot \frac{E_f \cdot E_c \cdot A_c}{E_c \cdot A_c + E_f \cdot A_f} \cdot \frac{d^2\delta}{dx^2} \tag{3.26}$$

that can be rewritten like:

$$\tau(x) = J_3 \cdot \frac{d^2\delta}{dx^2} \tag{3.27}$$

with:

$$J_3 = \frac{E_f \cdot A_f \cdot E_c \cdot A_c}{L_p \cdot (E_c \cdot A_c + E_f \cdot A_f)} \tag{3.28}$$

4 Local bond-stress-slip relationship

The local bond stress-slip relationship herein proposed to simulate the subsequent phases undergone by bond during the loading process is composed of four different linear branches (Fig. 4.1). Those phases, representing the physical phenomena occurring in sequence within the adhesive layer by increasing the imposed end slip, are: "elastic", "softening", "softening friction" and "free slipping".

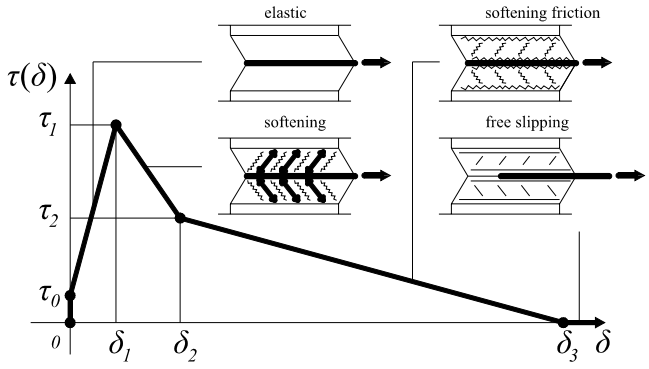

Fig. 4.1 – Proposed local bond stress-slip relationship: relevant phases of the failure occurring within the adhesive layer.

The first rigid branch represents the overall initial shear strength of the joint, independent of the deformability of the adhesive layer and attributable to the micro-mechanical and chemical properties of the involved materials and interfaces. In fact, the parameter τ_0 is the average of the following physical entities encountered in sequence by forces flowing from the strip to the surrounding concrete, *i.e.*: adhesion at the interface between strip and adhesive, cohesion within the adhesive itself and adhesion at the interface between adhesive and concrete. Up to the peak strength τ_1, a macro-mechanical strength due to the adhesive layer deformability adds to the constant adhesive-cohesive strength. That macro-mechanical strength due to the deformability of the intact adhesive layer can be conveniently modeled by a linear elastic behavior. Approaching the peak strength, the adhesive fractures along diagonal planes orthogonal to the traction isostatics as outlined by Sena-Cruz and Barros (2004) by means of post-test optical microscope photos. During the subsequent softening phase, force is transferred from the strip to the surrounding concrete by the resulting diagonal micro-struts. Anyway, throughout the softening phase, by increasing the imposed slip, concrete present at the extremities of those struts progressively deteriorates so as, increasing the imposed slip, micro-cracks parallel to the strip start to appear at both the strip-adhesive and adhesive-concrete interfaces. Approaching the softening friction phase, the resisting mechanism is gradually substituted by friction and micro-mechanical interlock along those resulting micro-cracks. Nonetheless, even those mechanisms undergo softening due to progressive material degradation. When even the resisting force provided by friction has exhausted, those micro-cracks result smooth discontinuities. The free slipping phase follows, during which the strip goes on being pulled out without having to overcome any opposing restraint left. For computational ease, also the softening and softening frictional behaviors are modelled as linear. The resulting analytical relationship is the following:

$$\tau(\delta)=\begin{cases}\tau_0+\dfrac{\tau_1-\tau_0}{\delta_1}\cdot\delta & 0\le\delta\le\delta_1\\ \tau_1-\dfrac{\tau_1-\tau_2}{\delta_2-\delta_1}\cdot(\delta-\delta_1) & \delta_1<\delta\le\delta_2\\ \tau_2-\dfrac{\tau_2}{\delta_3-\delta_2}\cdot(\delta-\delta_2) & \delta_2<\delta\le\delta_3\\ 0 & \delta>\delta_3\end{cases} \tag{4.1}$$

Among those parameters defining the local bond stress-slip relationship, the adhesive-cohesive term τ_0 is the one that more markedly depends on the micro-mechanical and chemical properties of the composite, of the adhesive and the concrete surfaces. For a better characterization of the influence of those aspects, a closer scale investigation is deemed as necessary. Moreover, all of the parameters defining the local bond stress-slip relationship should not be considered as having universally valid values but, on the contrary, should be determined on the basis of the mechanical-chemical and geometrical parameters characterizing the specific case at hand. Hereinafter, the entire debonding process is described deriving the relevant analytical expressions and referring to a classical push-pull test of an NSM CFRP laminate.

5 Debonding process for an infinite bond length

The entire debonding process affecting the behavior of an NSM strip is herein described distinguishing the several successive phases and referring to an infinite bond length. Those phases are singled out according to the value of the imposed slip and with respect to the assumed local bond stress-slip relationship.

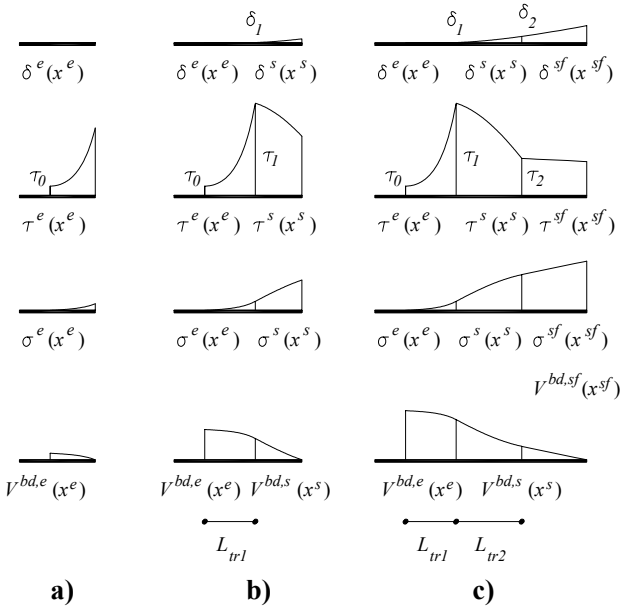

Fig. 5.1 – Debonding process for an infinite bond length: distribution of slip, bond stress, laminate axial stress and force transferred to the surrounding concrete along the transfer length for the bond phases: elastic a), softening b) and softening friction c).

5.1 First phase: elastic

When the imposed slip in the loaded end δ_{Li} is smaller than δ_1 *i.e.* if $\delta_{Li} \le \delta_1$, the governing differential equation (Eq. 3.16) solved in the local reference system ox^e originating in the leftward unloaded extremity of the transfer length, becomes (see Fig. 5.1a):

$$\left[\frac{\delta_1}{\left(\tau_f - \tau_0\right) \cdot J_1}\right] \cdot \frac{d^2\delta^e}{dx^{e2}} - \delta^e = \left(J_1 \cdot \tau_0\right) \cdot \frac{\delta_1}{\left(\tau_f - \tau_0\right) \cdot J_1} \tag{5.1}$$

that can be rewritten as:

$$\frac{1}{\lambda^2} \cdot \frac{d^2\delta^e}{dx^{e2}} - \delta^e = \left(J_1 \cdot \tau_0\right) \cdot \frac{1}{\lambda^2} \tag{5.2}$$

that results to be a linear differential equation of the second order not homogeneous, with:

$$\frac{1}{\lambda^2} = \frac{\delta_1}{\left(\tau_f - \tau_0\right) \cdot J_1} \tag{5.3}$$

where the latter position is possible since we've assumed that $\tau_f > \tau_0$. If this latter hypothesis is abandoned, *i.e.* if $\tau_f \le \tau_0$, Eq. 5.3 is no longer valid and the following equations should be conveniently modified.

The homogeneous associated to Eq. 5.2, by introducing the position $\delta^e = e^{u \cdot x^e}$ yields the following characteristic equation (Kreyszig 1998):

$$\frac{1}{\lambda^2} \cdot u^2 - 1 = 0 \tag{5.4}$$

that has solutions:

$$u_{1/2} = \pm\lambda \tag{5.5}$$

The general solution of Eq. 5.2, obtained by adding a particular solution of Eq. 5.2 to the solution of the homogenous associated is:

$$\delta^e\left(x^e\right) = C_1^e \cdot e^{\lambda \cdot x^e} + C_2^e \cdot e^{-\lambda \cdot x^e} - \frac{\tau_0 \cdot J_1}{\lambda^2} \tag{5.6}$$

and the relevant boundary conditions are:

$$\begin{cases} \delta^e = 0 \text{ at } x^e = 0 \\ \delta^e = \delta_{Li} \text{ at } x^e = L_{tr}^e\left(\delta_{Li}\right) \end{cases} \tag{5.7}$$

that, after substitution, become:

$$\begin{cases} C_1^e + C_2^e = \dfrac{\tau_0 \cdot J_1}{\lambda^2} \\ C_1^e \cdot e^{\lambda \cdot L_{tr}^e} + C_2^e \cdot e^{-\lambda \cdot L_{tr}^e} - \dfrac{\tau_0 \cdot J_1}{\lambda^2} = \delta_{Li} \end{cases} \tag{5.8}$$

Solving the system of equations Eq. 5.8, the expressions of the above constants can be obtained like follows:

$$C_1^e = \left[\delta_{Li} + \frac{\tau_0 \cdot J_1}{\lambda^2} \cdot \left(1 - e^{-\lambda \cdot L_{tr}^e} \right) \right] \cdot \frac{1}{e^{\lambda \cdot L_{tr}^e} - e^{-\lambda \cdot L_{tr}^e}} \tag{5.9}$$

$$C_2^e = \frac{\tau_0 \cdot J_1}{\lambda^2} - C_1^e \tag{5.10}$$

And the first and second order derivatives of Eq. 5.6:

$$\frac{d\delta^e}{dx^e} = C_1^e \cdot \lambda \cdot e^{\lambda \cdot x^e} - C_2^e \cdot \lambda \cdot e^{-\lambda \cdot x^e} \tag{5.11}$$

$$\frac{d^2\delta^e}{dx^{e^2}} = C_1^e \cdot \lambda^2 \cdot e^{\lambda \cdot x^e} + C_2^e \cdot \lambda^2 \cdot e^{-\lambda \cdot x^e} \tag{5.12}$$

From which the expression for determining the strip axial stress and the tangential stress along the strip can be determined as follows:

$$\sigma^e\left(x^e\right) = J_2 \cdot \left[C_1^e \cdot \lambda \cdot e^{\lambda \cdot x^e} - C_2^e \cdot \lambda \cdot e^{-\lambda \cdot x^e} \right] \tag{5.13}$$

$$\tau^e\left(x^e\right) = J_3 \cdot \left[C_1^e \cdot \lambda^2 \cdot e^{\lambda \cdot x^e} + C_2^e \cdot \lambda^2 \cdot e^{-\lambda \cdot x^e} \right] \tag{5.14}$$

The expression of the transfer length as function of the imposed slip can be obtained by imposing the following equilibrium condition:

$$L_p \cdot \int_0^{L_{tr}^e} \tau^e\left(x^e\right) \cdot dx^e = A_f \cdot \sigma_f\left(L_{tr}^e\right) \tag{5.15}$$

Substituting the relevant quantities, the left-hand member of Eq. 5.15 becomes:

$$L_p \cdot J_3 \cdot \left[\frac{d\delta^e}{dx^e} \right]_0^{L_{tr}^e} = \frac{A_f \cdot E_f \cdot A_c \cdot E_c}{A_f \cdot E_f + A_c \cdot E_c} \cdot \left[C_1^e \cdot \lambda \cdot e^{\lambda \cdot L_{tr}^e} - C_2^e \cdot \lambda \cdot e^{-\lambda \cdot L_{tr}^e} - C_1^e \cdot \lambda + C_2^e \cdot \lambda \right] \tag{5.16}$$

And the right-hand member:

$$A_f \cdot \sigma_f\left(L_{tr}^e\right) = A_f \cdot J_2 \cdot \left.\frac{d\delta^e}{dx^e}\right|_{L_{tr}^e} = \frac{A_f \cdot E_f \cdot A_c \cdot E_c}{A_f \cdot E_f + A_c \cdot E_c} \cdot \left[C_1^e \cdot \lambda \cdot e^{\lambda \cdot L_{tr}^e} - C_2^e \cdot \lambda \cdot e^{-\lambda \cdot L_{tr}^e}\right] \tag{5.17}$$

Thus, by considering the above Eqs. 5.16 and 5.17, Eq. 5.15 becomes:

$$C_1^e \cdot \lambda + C_2^e \cdot \lambda = 0 \tag{5.18}$$

that, after substituting the expressions of the constants as functions of the imposed slip yields:

$$\begin{aligned} &-\frac{1}{e^{\lambda \cdot L_{tr}^e} - e^{-\lambda \cdot L_{tr}^e}} \cdot \left[\delta_{Li} + \frac{\tau_0 \cdot J_1}{\lambda^2} \cdot \left(1 - e^{-\lambda \cdot L_{tr}^e}\right)\right] + \\ &\lambda \cdot \left\{\frac{\tau_0 \cdot J_1}{\lambda^2} - \frac{1}{e^{\lambda \cdot L_{tr}^e} - e^{-\lambda \cdot L_{tr}^e}} \cdot \left[\delta_{Li} + \frac{\tau_0 \cdot J_1}{\lambda^2} \cdot \left(1 - e^{-\lambda \cdot L_{tr}^e}\right)\right]\right\} = 0 \end{aligned} \tag{5.19}$$

The above Eq. 5.19 yields:

$$-\frac{2}{e^{\lambda \cdot L_{tr}^e} - e^{-\lambda \cdot L_{tr}^e}} \cdot \left[\delta_{Li} + \frac{\tau_0 \cdot J_1}{\lambda^2} \cdot \left(1 - e^{-\lambda \cdot L_{tr}^e}\right)\right] + \lambda \cdot \frac{\tau_0 \cdot J_1}{\lambda^2} = 0 \tag{5.20}$$

and, it can be rewritten as:

$$A^e \cdot e^{\lambda \cdot L_{tr}^e} + A^e \cdot e^{-\lambda \cdot L_{tr}^e} = B^e \tag{5.21}$$

with:

$$A^e = \frac{\tau_0 \cdot J_1}{2 \cdot \lambda^2} \tag{5.22}$$

$$B^e = \delta_{Li} + \frac{\tau_0 \cdot J_1}{\lambda^2} \tag{5.23}$$

And, introducing the hyperbolic cosine, Eq. 5.21 can be rewritten as:

$$2 \cdot A^e \cdot \cosh\left(\lambda \cdot L_{tr}^e\right) = B^e \tag{5.24}$$

from which it can be derived:

$$L_{tr}\left(\delta_{Li}\right) = L_{tr}^e\left(\delta_{Li}\right) = \frac{1}{\lambda} \cdot \operatorname{arcosh} \frac{B^e}{2 \cdot A^e} \tag{5.25}$$

The value of force transferred by bond to the surrounding concrete, along the transfer length $L_{tr}^e\left(\delta_{Li}\right)$ can be determined like follows:

$$V^{bd,e}\left(\delta_{Li}\right) = L_p \cdot \int_0^{L_{tr}^e} \tau^e\left(x^e\right) \cdot dx^e \tag{5.26}$$

The transfer length at the end of the elastic phase L_{tr1} and the corresponding value of force transferred to concrete V_1^{bd}, both invariants for given input parameters, are obtained respectively by Eq. 5.25 and 5.26 imposing $\delta_{Li} = \delta_1$:

$$V_1^{bd} = V^{bd,e}\left(\delta_1\right) \text{ and } L_{tr1} = L_{tr}^e\left(\delta_1\right) \tag{5.27}$$

5.2 Second phase: softening

When the imposed slip is $\delta_1 < \delta_{Li} \le \delta_2$ the solving differential equation, limited to the amount of the total transfer length being in the softening phase, becomes (see Fig. 5.1b):

$$\frac{1}{\beta^2} \cdot \frac{d^2\delta^s}{dx^{s^2}} + \delta^s = \frac{\tau_1 \cdot J_1}{\beta^2} + \delta_1 \tag{5.28}$$

with:

$$\frac{1}{\beta^2} = \frac{\left(\delta_2 - \delta_1\right)}{\left(\tau_1 - \tau_2\right) \cdot J_1} \tag{5.29}$$

The homogeneous associated to Eq. 5.28 yields, after assuming $\delta^s = e^{u \cdot x^s}$, the following characteristic equation:

$$\frac{1}{\beta^2} \cdot u^2 + 1 = 0 \tag{5.30}$$

with solution:

$$u_{1/2} = \pm\beta \cdot i \tag{5.31}$$

and the solution of the homogeneous results to be:

$$\delta^s = C_1^s \cdot \sin\left(\beta \cdot x^s\right) + C_2^s \cdot \cos\left(\beta \cdot x^s\right) \tag{5.32}$$

A particular solution of Eq. 5.28 is:

$$\delta^s = \frac{\tau_1 \cdot J_1}{\beta^2} + \delta_1 \tag{5.33}$$

Thus, the general solution of Eq. 5.28 is given by:

$$\delta^s\left(x^s\right)=C_1^s\cdot\sin\left(\beta\cdot x^s\right)+C_2^s\cdot\cos\left(\beta\cdot x^s\right)+\frac{\tau_1\cdot J_1}{\beta^2}+\delta_1 \tag{5.34}$$

and the boundary conditions, for a reference system ox^s that originates at the point of the bond length in correspondence of which slip results equal to δ_1, are:

$$\begin{cases}\delta^s=\delta_1 \text{ at } x^s=0\\ \delta^s=\delta_{Li} \text{ at } x^s=L_{tr}^s\end{cases} \tag{5.35}$$

From the above system of equations, Eq. 5.35, by substituting Eq. 5.34, it results:

$$C_1^s=\frac{1}{\sin\left(\beta\cdot L_{tr}^s\right)}\cdot\left\{\delta_{Li}-\delta_1+\frac{\tau_1\cdot J_1}{\beta^2}\cdot\left[\cos\left(\beta\cdot L_{tr}^s\right)-1\right]\right\} \tag{5.36}$$

$$C_2^s=-\frac{\tau_1\cdot J_1}{\beta^2} \tag{5.37}$$

The first and second order derivatives of Eq. 5.34:

$$\frac{d\delta^s}{dx^s}=C_1^s\cdot\beta\cdot\cos\left(\beta\cdot x^s\right)-C_2^s\cdot\beta\cdot\sin\left(\beta\cdot x^s\right) \tag{5.38}$$

$$\frac{d^2\delta^s}{dx^{s\,2}}=-C_1^s\cdot\beta^2\cdot\sin\left(\beta\cdot x^s\right)-C_2^s\cdot\beta^2\cdot\cos\left(\beta\cdot x^s\right) \tag{5.39}$$

From which the expression for determining the strip axial stress and the tangential stress along the strip can be determined as follows:

$$\sigma^s\left(x^s\right)=J_2\cdot\left[C_1^s\cdot\beta\cdot\cos\left(\beta\cdot x^s\right)-C_2^s\cdot\beta\cdot\sin\left(\beta\cdot x^s\right)\right] \tag{5.40}$$

$$\tau^s\left(x^s\right)=J_3\cdot\left[-C_1^s\cdot\beta^2\cdot\sin\left(\beta\cdot x^s\right)-C_2^s\cdot\beta^2\cdot\cos\left(\beta\cdot x^s\right)\right] \tag{5.41}$$

By imposing the following equilibrium condition:

$$V_1^{bd}+L_p\cdot\int_0^{L_{tr}^s}\tau^s\left(x^s\right)\cdot dx^s=A_f\cdot\sigma_f\left(L_{tr}^s\right) \tag{5.42}$$

the following equation for determining the amount of transfer length undergoing softening as function of the imposed slip can be obtained:

$$A^s\cdot\sin\left(\beta\cdot L_{tr}^s\right)-B^s\cdot\cos\left(\beta\cdot L_{tr}^s\right)=C^s \tag{5.43}$$

with:

$$A^s = V_1^{bd} \tag{5.44}$$

$$B^s = J_3 \cdot L_p \cdot \frac{\tau_1 \cdot J_1}{\beta} \tag{5.45}$$

$$C^s = J_3 \cdot L_p \cdot \beta \cdot \left(\delta_{Li} - \delta_1 - \frac{\tau_1 \cdot J_1}{\beta^2} \right) \tag{5.46}$$

Eq. 5.43 is a linear trigonometric equation that can be solved by a tricky expedient *i.e.*: both sides can be divided by $\sqrt{A^{s\,2} + B^{s\,2}}$:

$$\frac{A^s}{\sqrt{A^{s\,2} + B^{s\,2}}} \cdot \sin\left(\beta \cdot L_{tr}^s\right) - \frac{B^s}{\sqrt{A^{s\,2} + B^{s\,2}}} \cdot \cos\left(\beta \cdot L_{tr}^s\right) = \frac{C^s}{\sqrt{A^{s\,2} + B^{s\,2}}} \tag{5.47}$$

It can be easily observed that the following expressions are valid:

$$\cos\varphi = \frac{A^s}{\sqrt{A^{s\,2} + B^{s\,2}}} \tag{5.48}$$

$$\sin\varphi = \frac{B^s}{\sqrt{A^{s\,2} + B^{s\,2}}} \tag{5.49}$$

Thus, former Eq. 5.47 can be rewritten as:

$$\cos\varphi \cdot \sin\left(\beta \cdot L_{tr}^s\right) - \sin\varphi \cdot \cos\left(\beta \cdot L_{tr}^s\right) = \frac{C^s}{\sqrt{A^{s\,2} + B^{s\,2}}} \tag{5.50}$$

from which it descends:

$$\sin\left(\beta \cdot L_{tr}^s - \varphi\right) = \frac{C^s}{\sqrt{A^{s\,2} + B^{s\,2}}} \tag{5.51}$$

and the expression of the transfer length $L_{tr}^s\left(\delta_{Li}\right)$ corresponding to the amount of the infinite bond length undergoing softening can be obtained:

$$L_{tr}^s\left(\delta_{Li}\right) = \frac{1}{\beta} \cdot \left[\varphi + \arcsin \frac{C^s}{\sqrt{\left(A^s\right)^2 + \left(B^s\right)^2}} \right] \tag{5.52}$$

The overall transfer length, for $\delta_1 < \delta_{Li} \le \delta_2$, results to be:

$$L_{tr}\left(\delta_{Li}\right) = L_{tr1} + L_{tr}^s\left(\delta_{Li}\right) \tag{5.53}$$

and the value of force transferred by bond to the surrounding concrete:

$$V^{bd}\left(\delta_{Li}\right)=V_1^{bd}+V^{bd,s}\left(\delta_{Li}\right)=V_1^{bd}+L_p\cdot\int_0^{L_{tr}^s}\tau^s\left(x^s\right)\cdot dx^s \tag{5.54}$$

The maximum value of the transfer length that can be subject to softening and the relevant value of the force transferred to the surrounding concrete are the following invariants:

$$L_{tr2}=L_{tr}^s\left(\delta_2\right)\ \text{ and }\ V_2^{bd}=V^{bd,s}\left(\delta_2\right) \tag{5.55}$$

5.3 Third phase: softening friction

For an imposed end slip δ_{Li} resulting $\delta_2<\delta_{Li}\le\delta_3$ Eq. 3.16 becomes:

$$\frac{1}{\gamma^2}\cdot\frac{d^2\delta^{sf}}{dx^{sf\,2}}+\delta^{sf}\left(x^{sf}\right)=\delta_3 \tag{5.56}$$

with:

$$\frac{1}{\gamma^2}=\frac{\left(\delta_3-\delta_2\right)}{\tau_2\cdot J_1} \tag{5.57}$$

The characteristic equation of the homogeneous associated to Eq. 5.56 is:

$$\frac{1}{\gamma^2}\cdot u^2+1=0 \tag{5.58}$$

with solution:

$$u_{1/2}=\pm\gamma\cdot i \tag{5.59}$$

and the solution of the homogeneous results to be:

$$\delta^{sf}=C_1^{sf}\cdot\sin\left(\gamma\cdot x^{sf}\right)+C_2^{sf}\cdot\cos\left(\gamma\cdot x^{sf}\right) \tag{5.60}$$

A particular solution of Eq. 5.56 is:

$$\delta^{sf}=\delta_3 \tag{5.61}$$

Thus, the general solution of Eq. 5.56 is given by:

$$\delta^{sf}\left(x^{sf}\right)=C_1^{sf}\cdot\sin\left(\gamma\cdot x^{sf}\right)+C_2^{sf}\cdot\cos\left(\gamma\cdot x^{sf}\right)+\delta_3 \tag{5.62}$$

and the boundary conditions, for a reference system ox^{sf} that originates at the point of the infinite bond length in correspondence of which slip results equal to δ_2, are:

$$\begin{cases} \delta^{sf} = \delta_2 \ \text{ at } \ x^{sf} = 0 \\ \delta^{sf} = \delta_{Li} \ \text{ at } \ x^{sf} = L_{tr}^{sf} \end{cases} \tag{5.63}$$

From the above system of equations, Eq. 5.35, by substituting Eq. 5.34, it results:

$$C_1^{sf} = \frac{1}{\sin\left(\gamma \cdot L_{tr}^{sf}\right)} \cdot \left[\delta_{Li} - \delta_3 + \left(\delta_3 - \delta_2\right) \cdot \cos\left(\gamma \cdot L_{tr}^{sf}\right)\right] \tag{5.64}$$

$$C_2^{sf} = \delta_2 - \delta_3 \tag{5.65}$$

The first and second order derivatives of Eq. 5.62:

$$\frac{d\delta^{sf}}{dx^{sf}} = C_1^{sf} \cdot \gamma \cdot \cos\left(\gamma \cdot x^{sf}\right) - C_2^{sf} \cdot \gamma \cdot \sin\left(\gamma \cdot x^{sf}\right) \tag{5.66}$$

$$\frac{d^2\delta^{sf}}{dx^{sf\,2}} = -C_1^{sf} \cdot \gamma^2 \cdot \sin\left(\gamma \cdot x^{sf}\right) - C_2^{sf} \cdot \gamma^2 \cdot \cos\left(\gamma \cdot x^{sf}\right) \tag{5.67}$$

From which the expression for determining the strip axial stress and the tangential stress along the strip can be determined as follows:

$$\sigma^{sf}\left(x^{sf}\right) = J_2 \cdot \left[C_1^{sf} \cdot \gamma \cdot \cos\left(\gamma \cdot x^{sf}\right) - C_2^{sf} \cdot \gamma \cdot \sin\left(\gamma \cdot x^{sf}\right)\right] \tag{5.68}$$

$$\tau^{sf}\left(x^{sf}\right) = J_3 \cdot \left[-C_1^{sf} \cdot \gamma^2 \cdot \sin\left(\gamma \cdot x^{sf}\right) - C_2^{sf} \cdot \gamma^2 \cdot \cos\left(\gamma \cdot x^{sf}\right)\right] \tag{5.69}$$

By imposing the following equilibrium condition:

$$V_1^{bd} + V_2^{bd} + L_p \cdot \int_0^{L_{tr}^{sf}} \tau^{sf}\left(x^{sf}\right) \cdot dx^{sf} = A_f \cdot \sigma_f\left(L_{tr}^{sf}\right) \tag{5.70}$$

the following equation for determining the amount of transfer length undergoing softening friction as function of the imposed slip can be obtained:

$$A^{sf} \cdot \sin\left(\gamma \cdot L_{tr}^{sf}\right) - B^{sf} \cdot \cos\left(\gamma \cdot L_{tr}^{sf}\right) = C^{sf} \tag{5.71}$$

with:

$$A^{sf} = V_1^{bd} + V_2^{bd} \tag{5.72}$$

$$B^{sf} = J_3 \cdot L_p \cdot \gamma \cdot \left(\delta_3 - \delta_2\right) \tag{5.73}$$

$$C^{sf} = J_3 \cdot L_p \cdot \gamma \cdot \left(\delta_{Li} - \delta_3\right) \tag{5.74}$$

Eq. 5.71 is a linear trigonometric equation that can be solved by a tricky expedient *i.e.*: both sides can be divided by $\sqrt{A^{sf\,2}+B^{sf\,2}}$:

$$\frac{A^{sf}}{\sqrt{A^{sf\,2}+B^{sf\,2}}}\cdot\sin\left(\gamma\cdot L_{tr}^{sf}\right)-\frac{B^{sf}}{\sqrt{A^{sf\,2}+B^{sf\,2}}}\cdot\cos\left(\gamma\cdot L_{tr}^{sf}\right)=\frac{C^{sf}}{\sqrt{A^{sf\,2}+B^{sf\,2}}} \tag{5.75}$$

It can be easily observed that the following expressions are valid:

$$\cos\psi=\frac{A^{sf}}{\sqrt{A^{sf\,2}+B^{sf\,2}}} \tag{5.76}$$

$$\sin\psi=\frac{B^{sf}}{\sqrt{A^{sf\,2}+B^{sf\,2}}} \tag{5.77}$$

Thus, former Eq. 5.75 can be rewritten as:

$$\cos\psi\cdot\sin\left(\gamma\cdot L_{tr}^{sf}\right)-\sin\psi\cdot\cos\left(\gamma\cdot L_{tr}^{sf}\right)=\frac{C^{sf}}{\sqrt{A^{sf\,2}+B^{sf\,2}}} \tag{5.78}$$

from which it descends:

$$\sin\left(\gamma\cdot L_{tr}^{sf}-\psi\right)=\frac{C^{sf}}{\sqrt{A^{sf\,2}+B^{sf\,2}}} \tag{5.79}$$

and the expression of the transfer length $L_{tr}^{sf}\left(\delta_{Li}\right)$ corresponding to the amount of the infinite bond length undergoing softening can be obtained:

$$L_{tr}^{sf}\left(\delta_{Li}\right)=\frac{1}{\gamma}\cdot\left[\psi+\arcsin\frac{C^{sf}}{\sqrt{\left(A^{sf}\right)^2+\left(B^{sf}\right)^2}}\right]\ \text{with}\ \psi=\arcsin\frac{B^{sf}}{\sqrt{\left(A^{sf}\right)^2+\left(B^{sf}\right)^2}} \tag{5.80}$$

The overall transfer length, for $\delta_1<\delta_{Li}\le\delta_2$, results to be:

$$L_{tr}\left(\delta_{Li}\right)=L_{tr1}+L_{tr2}+L_{tr}^{sf}\left(\delta_{Li}\right) \tag{5.81}$$

and the value of force transferred by bond to the surrounding concrete:

$$V^{bd}\left(\delta_{Li}\right)=V_1^{bd}+V_2^{bd}+V^{bd,sf}\left(\delta_{Li}\right)=V_1^{bd}+V_2^{bd}+L_p\cdot\int_0^{L_{tr}^{sf}}\tau^{sf}\left(x^{sf}\right)\cdot dx^{sf} \tag{5.82}$$

The maximum value of the transfer length that can be subject to softening and the relevant value of the force transferred to the surrounding concrete are the following invariants:

$$L_{tr2} = L_{tr}^{s}\left(\delta_2\right) \text{ and } V_2^{bd} = V^{bd,s}\left(\delta_2\right) \tag{5.83}$$

The maximum value of the infinite bond length that can be subject to *softening friction* and the relevant value of the force transferred to the surrounding concrete are:

$$L_{tr3} = L_{tr}^{sf}\left(\delta_3\right) \text{ and } V_3^{bd} = V^{bd,sf}\left(\delta_3\right) \tag{5.84}$$

5.4 Fourth phase: free slipping

When the imposed slip is larger than the value in correspondence of which *free slipping* begins, *i.e.* if it is $\delta_{Li} > \delta_3$, the solving differential equation becomes (see Fig. 5.2):

$$\frac{d^2\delta^{fs}}{dx^{fs\,2}} = 0 \tag{5.85}$$

The expression for the interfacial slip is:

$$\delta^{fs}\left(x^{fs}\right) = C_1^{fs} \cdot x^{fs} + C_2^{fs} \tag{5.86}$$

and the boundary conditions, for a reference system ox^{fs} that originates at the point of the bond length in correspondence of which slip results equal to δ_3, are:

$$\begin{cases} \delta^{fs} = \delta_3 \text{ at } x^{fs} = 0 \\ \delta^{fs} = \delta_{Li} \text{ at } x^{fs} = L_{tr}^{fs} \end{cases} \tag{5.87}$$

The constants of integration are:

$$C_1^{fs} = \frac{\delta_{Li} - \delta_3}{L_{tr}^{fs}} \tag{5.88}$$

$$C_2^{fs} = \delta_3 \tag{5.89}$$

The first and second order derivatives of Eq. 5.86:

$$\frac{d\delta^{fs}}{dx^{fs}} = C_1^{fs} \tag{5.90}$$

$$\frac{d^2\delta^{fs}}{dx^{fs\,2}} = 0 \tag{5.91}$$

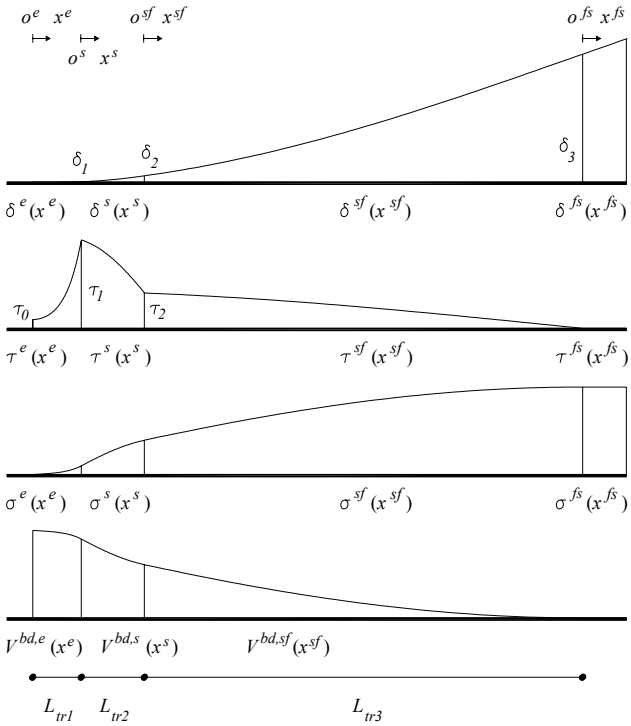

Fig. 5.2 – Free Slipping phase of the debonding process for an infinite bond length: distribution of slip, bond stress, strip axial stress and force transferred to the surrounding concrete along the transfer length.

From Eqs. 5.90 and 5.91, the expression for determining the strip axial stress and the tangential stress along the strip can be determined as follows:

$$\sigma^{fs}\left(x^{fs}\right) = J_2 \cdot C_1^{fs} = \text{constant} \tag{5.92}$$

$$\tau^{fs}\left(x^{fs}\right) = 0 \tag{5.93}$$

By imposing the following equilibrium condition:

$$V_1^{bd} + V_2^{bd} + V_3^{bd} = A_f \cdot \sigma^{fs}\left(L_{tr}^{fs}\right) \tag{5.94}$$

the following equation for determining the amount of transfer length $L_{tr}^{fs}\left(\delta_{Li}\right)$ undergoing softening friction as function of the imposed slip can be obtained:

$$L_{tr}^{fs}\left(\delta_{Li}\right) = J_3 \cdot L_p \cdot \frac{\delta_{Li} - \delta_3}{V_1^{bd} + V_2^{bd} + V_3^{bd}} \tag{5.95}$$

The overall transfer length, for $\delta_{Li} > \delta_3$, results to be:

$$L_{tr}\left(\delta_{Li}\right) = L_{tr1} + L_{tr2} + L_{tr3} + L_{tr}^{fs}\left(\delta_{Li}\right) \tag{5.96}$$

and the value of force transferred by bond to the surrounding concrete:

$$V^{bd}\left(\delta_{Li}\right) = V_1^{bd} + V_2^{bd} + V_3^{bd} \tag{5.97}$$

6 Debonding process for a finite bond length

Once the constants defining the debonding process have been determined as above specified based on the input parameters ($a_f; b_f; E_f; a_c; b_c; E_c; \tau_0; \tau_1; \tau_2; \delta_1; \delta_2; \delta_3$), the values of the transfer length $L_{tr,i}\left(L_{Rfi}; \delta_{Li}\right)$, the corresponding force $V_{fi}^{bd}\left(L_{Rfi}; \delta_{Li}\right)$ transferred by bond for an imposed slip δ_{Li} and its progressive value along the transfer length $V_{fi}^{bd}\left(L_{Rfi}; \delta_{Li}; x_i^{tr}\right)$ can be determined for whatever value of the resisting bond length L_{Rfi} as hereafter specified. Debonding propagation can be thought of as a constant "wave" progressing from the loaded end inward towards the free extremity of the NSM strip, see Fig. (6.1a).

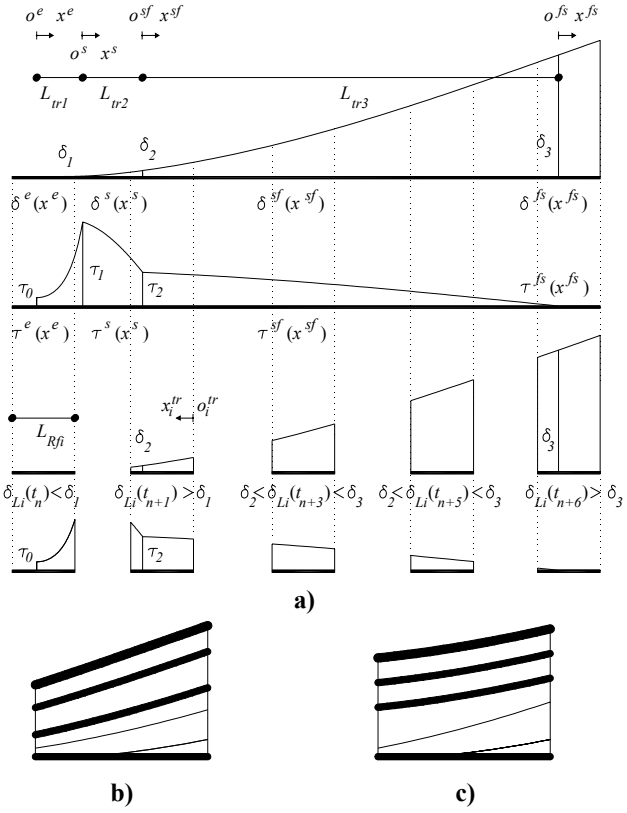

Fig. 6.1 – Debonding process for a finite bond length: "bond wave" progressing towards the free end (a); analytical increasing rate for free and loaded end slips (b) and experimental trend (qualitative) (c).

According to the present formulation, after slip propagation has reached the free extremity, initially the free end slip goes on increasing with a lower rate with respect to the imposed slip and successively they continue to increase with the same rate. This is shown by Fig. 6.1b, in which progressively thicker lines represent slip distribution along the bond length for increasing values of the imposed slip. Actually, experimental evidence (Sena-Cruz 2004, Sena-Cruz and Barros 2004) showed that, after the slip started to be felt at the free extremity, it first increased with a lower rate with

respect to the loaded end one, than with a higher rate and finally they increased with the same rate (Fig. 6.1c). That phenomenon can be ascribed to the elastic recover of the strip along the softening phase. Anyway, neglecting that aspect is deemed a reasonable compromise between accuracy and computational ease. Hereinafter, the analytical expressions for calculating the transfer length $L_{tr,i}$, the bond transferred force V_{fi}^{bd}, the free end slip δ_{Fi} and the progressive value $V_{fi}^{bd}\left(x_i^{tr}\right)$ of force transferred to the surrounding concrete as function of the imposed slip δ_{Li} are derived.

6.1 First phase: elastic

If the imposed slip is $0 < \delta_{Li} \le \delta_1$ the corresponding value of $L_{tr}\left(\delta_{Li}\right)$ is calculated by Eq. 5.25 and then, if $L_{Rfi} \ge L_{tr}\left(\delta_{Li}\right)$, it is (cases *a-d* in Fig. 6.2):

$$\begin{cases} L_{tr,i}\left(L_{Rfi};\delta_{Li}\right) = L_{tr}\left(\delta_{Li}\right) \\ V_{fi}^{bd}\left(L_{Rfi};\delta_{Li}\right) = L_p \cdot \int_0^{x_2^e} \tau^e\left(x^e\right)\cdot dx^e \\ x_2^e = L_{tr}\left(\delta_{Li}\right) \\ \delta_{Fi}\left(L_{Rfi};\delta_{Li}\right) = 0 \\ V_{fi}^{bd}\left(x_i^{tr}\right) = L_p \cdot \int_{L_{tr}(\delta_{Li})-x_i^{tr}}^{x_2^e} \tau^e\left(x^e\right)\cdot dx^e \quad \text{for} \quad 0 \le x_i^{tr} \le L_{tr,i}\left(L_{Rfi};\delta_{Li}\right) \end{cases} \tag{6.1}$$

and if $L_{Rfi} < L_{tr}\left(\delta_{Li}\right)$, it is (cases *e-f* in Fig. 6.2):

$$\begin{cases} L_{tr,i}\left(L_{Rfi};\delta_{Li}\right) = L_{Rfi} \\ V_{fi}^{bd}\left(L_{Rfi};\delta_{Li}\right) = \int_{x_1^h}^{x_2^e} \tau^e\left(x^e\right)\cdot dx^e \\ x_1^e = L_{tr}\left(\delta_{Li}\right) - L_{Rfi} \quad \text{and} \quad x_2^e = L_{tr}\left(\delta_{Li}\right) \\ \delta_{Fi}\left(L_{Rfi};\delta_{Li}\right) = \delta^e\left(x_1^e\right) \\ V_{fi}^{bd}\left(x_i^{tr}\right) = L_p \cdot \int_{L_{tr}(\delta_{Li})-x_i^{tr}}^{x_2^e} \tau^e\left(x^e\right)\cdot dx^e \quad \text{for} \quad 0 \le x_i^{tr} \le L_{tr,i}\left(L_{Rfi};\delta_{Li}\right) \end{cases} \tag{6.2}$$

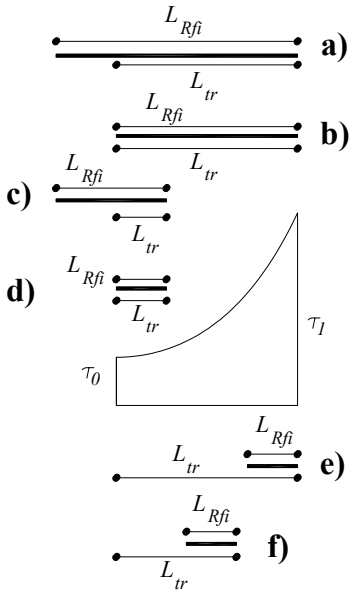

Fig. 6.2 – Possible configurations of bond stress with respect to finite value of resisting bond length and relative transfer length for an imposed slip $0 \le \delta_{Li} \le \delta_1$.

6.2 Second phase: softening

If the imposed slip is $\delta_1 < \delta_{Li} \le \delta_2$ the corresponding value of $L_{tr}(\delta_{Li})$ is calculated by Eq. 5.53 and then, if $L_{Rfi} \ge L_{tr}(\delta_{Li})$, it is (cases *a-d* in Fig. 6.3):

$$
\begin{cases}
L_{tr,i}\left(L_{Rfi};\delta_{Li}\right) = L_{tr}\left(\delta_{Li}\right) \\
V_{fi}^{bd}\left(L_{Rfi};\delta_{Li}\right) = V_1^{bd} + L_p \cdot \int_0^{x_2^s} \tau^s\left(x^s\right)\cdot dx^s \\
x_2^s = L_{tr}\left(\delta_{Li}\right) - L_{tr1} \\
\delta_{Fi}\left(L_{Rfi};\delta_{Li}\right) = 0 \\
V_{fi}^{bd}\left(x_i^{tr}\right) = L_p \cdot \int_{L_{tr}(\delta_{Li})-\left(L_{tr1}+x_i^{tr}\right)}^{x_2^s} \tau^s\left(x^s\right)\cdot dx^s \qquad \text{for} \quad 0 \le x_i^{tr} \le x_2^s \\
V_{fi}^{bd}\left(x_i^{tr}\right) = L_p \cdot \left[\int_{L_{tr}(\delta_{Li})-x_i^{tr}}^{L_{tr1}} \tau^e\left(x^e\right)\cdot dx^e + \int_0^{x_2^s} \tau^s\left(x^s\right)\cdot dx^s\right] \quad \text{for} \quad x_2^s < x_i^{tr} \le L_{tr,i}\left(L_{Rfi};\delta_{Li}\right)
\end{cases}
\tag{6.3}
$$

If $L_{Rfi} < L_{tr}(\delta_{Li})$ and $L_{tr}(\delta_{Li}) - L_{Rfi} < L_{tr1}$, it is (cases e and h in Fig. 6.3):

$$\begin{cases} L_{tr,i}\left(L_{Rfi};\delta_{Li}\right)=L_{Rfi} \\ V_{fi}^{bd}\left(L_{Rfi};\delta_{Li}\right)=L_p\cdot\left[\displaystyle\int_{x_1^h}^{L_{tr1}}\tau^e\left(x^e\right)\cdot dx^e+\int_0^{x_2^s}\tau^s\left(x^s\right)\cdot dx^s\right] \\ x_1^h=L_{tr}\left(\delta_{Li}\right)-L_{Rfi}\ \text{ and }\ x_2^s=L_{tr}\left(\delta_{Li}\right)-L_{tr1} \\ \delta_{Fi}\left(L_{Rfi};\delta_{Li}\right)=\delta^e\left(x_1^e\right) \\ V_{fi}^{bd}\left(x_i^{tr}\right)=L_p\cdot\displaystyle\int_{L_{tr}(\delta_{Li})-\left(L_{tr1}+x_i^{tr}\right)}^{x_2^s}\tau^s\left(x^s\right)\cdot dx^s \qquad \text{for} \quad 0\le x_i^{tr}\le x_2^s \\ V_{fi}^{bd}\left(x_i^{tr}\right)=L_p\cdot\left[\displaystyle\int_{L_{tr}(\delta_{Li})-x_i^{tr}}^{L_{tr1}}\tau^e\left(x^e\right)\cdot dx^e+\int_0^{x_2^s}\tau^s\left(x^s\right)\cdot dx^s\right]\ \text{for}\ x_2^s<x_i^{tr}\le L_{tr,i}\left(L_{Rfi};\delta_{Li}\right) \end{cases} \tag{6.4}$$

If $L_{Rfi}<L_{tr}\left(\delta_{Li}\right)$ and $L_{tr}\left(\delta_{Li}\right)-L_{Rfi}\ge L_{tr1}$, it is (cases *f*, *g* and *i* in Fig. 6.3):

$$\begin{cases} L_{tr,i}\left(L_{Rfi};\delta_{Li}\right)=L_{Rfi} \\ V_{fi}^{bd}\left(L_{Rfi};\delta_{Li}\right)=L_p\cdot\displaystyle\int_{x_1^s}^{x_2^s}\tau^s\left(x^s\right)\cdot dx^s \\ x_1^s=L_{tr}\left(\delta_{Li}\right)-\left(L_{Rfi}+L_{tr1}\right)\ \textit{and}\ \ x_2^s=L_{tr}\left(\delta_{Li}\right)-L_{tr1} \\ \delta_{Fi}\left(L_{Rfi};\delta_{Li}\right)=\delta^s\left(x_1^s\right) \\ V_{fi}^{bd}\left(x_i^{tr}\right)=L_p\cdot\displaystyle\int_{L_{tr}(\delta_{Li})-\left(L_{tr1}+x_i^{tr}\right)}^{x_2^s}\tau^s\left(x^s\right)\cdot dx^s \quad \text{for} \quad 0\le x_i^{tr}\le L_{tr,i}\left(L_{Rfi};\delta_{Li}\right) \end{cases} \tag{6.5}$$

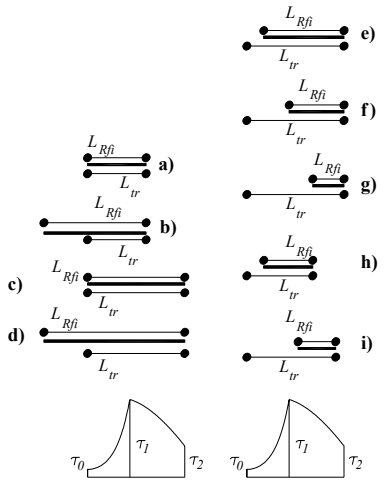

Fig. 6.3 – Possible configurations of bond stress with respect to finite resisting bond length and relative transfer length for an imposed slip $\delta_1 < \delta_{Li} \le \delta_2$.

6.3 Third phase: softening friction

If the imposed slip is $\delta_2 < \delta_{Li} \le \delta_3$, the corresponding value of $L_{tr}(\delta_{Li})$ is calculated by Eq. (4.81) and then, if $L_{Rfi} \ge L_{tr}(\delta_{Li})$ it is (cases *a* and *b* in Fig. 6.4):

$$
\begin{cases}
L_{tr,i}\left(L_{Rfi};\delta_{Li}\right)=L_{tr}\left(\delta_{Li}\right) \\
V_{fi}^{bd}\left(L_{Rfi};\delta_{Li}\right)=V_1^{bd}+V_2^{bd}+L_p\cdot\int_0^{x_2^{sf}}\tau^{sf}\left(x^{sf}\right)\cdot dx^{sf} \\
x_2^{sf}=L_{tr}\left(\delta_{Li}\right)-\left(L_{tr1}+L_{tr2}\right) \\
\delta_{Fi}\left(L_{Rfi};\delta_{Li}\right)=0
\end{cases}
$$

$$
\begin{cases}
V_{fi}^{bd}\left(x_i^{tr}\right)=L_p\cdot\int_{L_{tr}\left(\delta_{Li}\right)-\left(L_{tr1}+L_{tr2}+x_i^{tr}\right)}^{x_2^{sf}}\tau^{sf}\left(x^{sf}\right)\cdot dx^{sf} \qquad \text{for} \quad 0\le x_i^{tr}\le x_2^{sf} \\
V_{fi}^{bd}\left(x_i^{tr}\right)=L_p\cdot\left[\int_{L_{tr}\left(\delta_{Li}\right)-\left(L_{tr1}+x_i^{tr}\right)}^{L_{tr2}}\tau^{s}\left(x^{s}\right)\cdot dx^{s}+\int_0^{x_2^{sf}}\tau^{sf}\left(x^{sf}\right)\cdot dx^{sf}\right] \qquad \text{for} \quad x_2^{sf}<x_i^{tr}\le\left(x_2^{sf}+L_{tr2}\right) \\
V_{fi}^{bd}\left(x_i^{tr}\right)=L_p\cdot\left[\int_{L_{tr}\left(\delta_{Li}\right)-x_i^{tr}}^{L_{tr1}}\tau^{e}\left(x^{e}\right)\cdot dx^{e}+\int_0^{L_{tr2}}\tau^{s}\left(x^{s}\right)\cdot dx^{s}+\int_0^{x_2^{sf}}\tau^{sf}\left(x^{sf}\right)\cdot dx^{sf}\right]\ \ldots \\
\ldots\ \text{for}\ \left(x_2^{sf}+L_{tr2}\right)<x_i^{tr}\le L_{tr,i}\left(L_{Rfi};\delta_{Li}\right)
\end{cases}
\tag{6.6}
$$

If $L_{Rfi}<L_{tr}\left(\delta_{Li}\right)$ and $L_{tr}\left(\delta_{Li}\right)-L_{Rfi}<L_{tr1}$, it is (case *c* in Fig. 6.4) :

$$
\begin{cases}
L_{tr,i}\left(L_{Rfi};\delta_{Li}\right)=L_{Rfi} \\
V_{fi}^{bd}\left(L_{Rfi};\delta_{Li}\right)=V_2^{bd}+L_p\cdot\left[\displaystyle\int_{x_1^e}^{L_{tr}1}\tau^e\left(x^e\right)\cdot dx^e+\int_0^{x_2^{sf}}\tau^{sf}\left(x^{sf}\right)\cdot dx^{sf}\right] \\
x_1^e=L_{tr}\left(\delta_{Li}\right)-L_{Rfi}\ \text{ and }\ x_2^{sf}=L_{tr}\left(\delta_{Li}\right)-\left(L_{tr1}+L_{tr2}\right) \\
\delta_{Fi}\left(L_{Rfi};\delta_{Li}\right)=\delta^e\left(x_1^e\right)
\end{cases}
$$

$$
\begin{cases}
V_{fi}^{bd}\left(x_i^{tr}\right)=L_p\cdot\displaystyle\int_{L_{tr}\left(\delta_{Li}\right)-\left(L_{tr1}+L_{tr2}+x_i^{tr}\right)}^{x_2^{sf}}\tau^{sf}\left(x^{sf}\right)\cdot dx^{sf} \qquad \text{for}\quad 0\le x_i^{tr}\le x_2^{sf} \\
V_{fi}^{bd}\left(x_i^{tr}\right)=L_p\cdot\left[\displaystyle\int_{L_{tr}\left(\delta_{Li}\right)-\left(L_{tr1}+x_i^{tr}\right)}^{L_{tr}2}\tau^s\left(x^s\right)\cdot dx^s+\int_0^{x_2^{sf}}\tau^{sf}\left(x^{sf}\right)\cdot dx^{sf}\right] \qquad \text{for}\quad x_2^{sf}<x_i^{tr}\le\left(x_2^{sf}+L_{tr2}\right) \\
V_{fi}^{bd}\left(x_i^{tr}\right)=L_p\cdot\left[\displaystyle\int_{L_{tr}\left(\delta_{Li}\right)-x_i^{tr}}^{L_{tr}1}\tau^e\left(x^e\right)\cdot dx^e+\int_0^{L_{tr}2}\tau^s\left(x^s\right)\cdot dx^s+\int_0^{x_2^{sf}}\tau^{sf}\left(x^{sf}\right)\cdot dx^{sf}\right]\ \ldots \\
\ldots.\ \text{for}\ \left(x_2^{sf}+L_{tr2}\right)<x_i^{tr}\le L_{tr,i}\left(L_{Rfi};\delta_{Li}\right)
\end{cases}
\tag{6.7}
$$

If $L_{Rfi}<L_{tr}\left(\delta_{Li}\right)$ and $L_{tr1}\le L_{tr}\left(\delta_{Li}\right)-L_{Rfi}\le\left(L_{tr1}+L_{tr2}\right)$, it is (cases *d* and *e* in Fig. 6.4):

$$
\begin{cases}
L_{tr,i}\left(L_{Rfi};\delta_{Li}\right)=L_{Rfi} \\
V_{fi}^{bd}\left(L_{Rfi};\delta_{Li}\right)=L_p\cdot\left[\displaystyle\int_{x_1^s}^{L_{tr}2}\tau^s\left(x^s\right)\cdot dx^s+\int_0^{x_2^{sf}}\tau^{sf}\left(x^{sf}\right)\cdot dx^{sf}\right] \\
x_1^s=L_{tr}\left(\delta_{Li}\right)-\left(L_{Rfi}+L_{tr1}\right)\ \text{ and }\ x_2^{sf}=L_{tr}\left(\delta_{Li}\right)-\left(L_{tr1}+L_{tr2}\right) \\
\delta_{Fi}\left(L_{Rfi};\delta_{Li}\right)=\delta^s\left(x_1^s\right)
\end{cases}
$$

$$
\begin{cases}
V_{fi}^{bd}\left(x_i^{tr}\right)=L_p\cdot\displaystyle\int_{L_{tr}\left(\delta_{Li}\right)-\left(L_{tr1}+L_{tr2}+x_i^{tr}\right)}^{x_2^{sf}}\tau^{sf}\left(x^{sf}\right)\cdot dx^{sf} \qquad \text{for}\quad 0\le x_i^{tr}\le x_2^{sf} \\
V_{fi}^{bd}\left(x_i^{tr}\right)=L_p\cdot\left[\displaystyle\int_{L_{tr}\left(\delta_{Li}\right)-\left(L_{tr1}+x_i^{tr}\right)}^{L_{tr}2}\tau^s\left(x^s\right)\cdot dx^s+\int_0^{x_2^{sf}}\tau^{sf}\left(x^{sf}\right)\cdot dx^{sf}\right] \qquad \text{for}\quad x_2^{sf}<x_i^{tr}\le L_{tr,i}\left(L_{Rfi};\delta_{Li}\right)
\end{cases}
\tag{6.8}
$$

If $L_{Rfi} < L_{tr}(\delta_{Li})$ and $(L_{tr1} + L_{tr2}) < L_{tr}(\delta_{Li}) - L_{Rfi} \le (L_{tr1} + L_{tr2} + L_{tr3})$, it is (case *f* in Fig. 6.4):

$$\begin{cases} L_{tr,i}(L_{Rfi};\delta_{Li}) = L_{Rfi} \\ V_{fi}^{bd}(L_{Rfi};\delta_{Li}) = L_p \cdot \int_{x_1^{sf}}^{x_2^{sf}} \tau^{sf}(x^{sf}) \cdot dx^{sf} \\ x_1^{sf} = L_{tr}(\delta_{Li}) - (L_{tr1} + L_{tr2} + L_{Rfi}) \text{ and } x_2^{sf} = L_{tr}(\delta_{Li}) - (L_{tr1} + L_{tr2}) \\ \delta_{Fi}(L_{Rfi};\delta_{Li}) = \delta^{sf}(x_1^{sf}) \\ V_{fi}^{bd}(x_i^{tr}) = L_p \cdot \int_{L_{tr}(\delta_{Li}) - (L_{tr1} + L_{tr2} + x_i^{tr})}^{x_2^{sf}} \tau^{sf}(x^{sf}) \cdot dx^{sf} \quad \text{for} \quad 0 \le x_i^{tr} \le L_{tr,i}(L_{Rfi};\delta_{Li}) \end{cases} \tag{6.9}$$

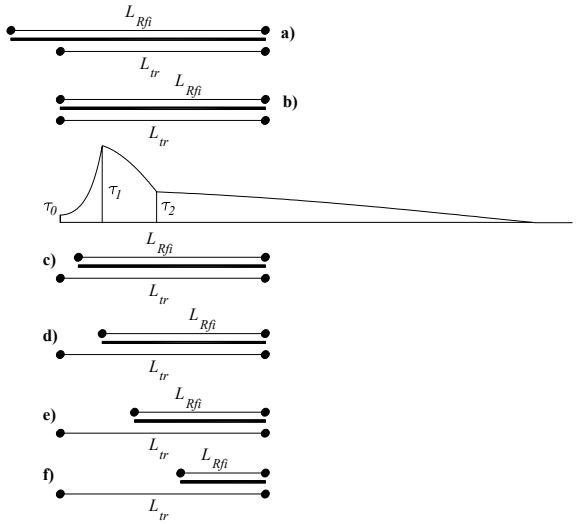

Fig. 6.4 – Possible configurations of bond stress with respect to finite resisting bond length and relative transfer length for an imposed slip $\delta_2 < \delta_{Li} \le \delta_3$.

6.4 Fourth phase: free slipping

If the imposed slip is $\delta_{Li} > \delta_3$, the corresponding value of $L_{tr}(\delta_{Li})$ is calculated by Eq. 5.95 and then, if $L_{Rfi} \ge L_{tr}(\delta_{Li})$ it is (cases *a* and *b* in Fig. 6.5):

$$
\begin{cases}
L_{tr,i}\left(L_{Rfi};\delta_{Li}\right)=L_{tr}\left(\delta_{Li}\right)\\
V_{fi}^{bd}\left(L_{Rfi};\delta_{Li}\right)=V_1^{bd}+V_2^{bd}+V_3^{bd}\\
\delta_{Fi}\left(L_{Rfi};\delta_{Li}\right)=0\\
x_2^{fs}=L_{tr}\left(\delta_{Li}\right)-\left(L_{tr1}+L_{tr2}+L_{tr3}\right)\\
\begin{cases}
V_{fi}^{bd}\left(x_i^{tr}\right)=0 \quad \text{for} \quad 0\le x_i^{tr}\le x_2^{fs}\\
V_{fi}^{bd}\left(x_i^{tr}\right)=L_p\cdot\displaystyle\int_{L_{tr}(\delta_{Li})-\left(L_{tr1}+L_{tr2}+x_i^{tr}\right)}^{L_{tr3}}\tau^{sf}\left(x^{sf}\right)\cdot dx^{sf} \quad \text{for} \quad x_2^{fs}<x_i^{tr}\le\left(x_2^{fs}+L_{tr3}\right)\\
V_{fi}^{bd}\left(x_i^{tr}\right)=L_p\cdot\left[\displaystyle\int_{L_{tr}(\delta_{Li})-\left(L_{tr1}+x_i^{tr}\right)}^{L_{tr2}}\tau^{s}\left(x^{s}\right)\cdot dx^{s}+\int_0^{L_{tr3}}\tau^{sf}\left(x^{sf}\right)\cdot dx^{sf}\right]....\\
.... \quad \text{for} \quad \left(x_2^{fs}+L_{tr3}\right)<x_i^{tr}\le\left(x_2^{fs}+L_{tr2}+L_{tr3}\right)\\
V_{fi}^{bd}\left(x_i^{tr}\right)=L_p\cdot\left[\displaystyle\int_{L_{tr}(\delta_{Li})-x_i^{tr}}^{L_{tr1}}\tau^{e}\left(x^{e}\right)\cdot dx^{e}+\int_0^{L_{tr2}}\tau^{s}\left(x^{s}\right)\cdot dx^{s}+\int_0^{L_{tr3}}\tau^{sf}\left(x^{sf}\right)\cdot dx^{sf}\right]...\\
.... \quad \text{for}\ \left(x_2^{fs}+L_{tr2}+L_{tr3}\right)<x_i^{tr}\le L_{tr,i}\left(L_{Rfi};\delta_{Li}\right)
\end{cases}
\end{cases}
\tag{6.10}
$$

If $L_{Rfi}<L_{tr}\left(\delta_{Li}\right)$ and $L_{tr}\left(\delta_{Li}\right)-L_{Rfi}<L_{tr1}$, it is (case *c* in Fig. 6.5):

$$
\begin{cases}
L_{tr,i}\left(L_{Rfi};\delta_{Li}\right)=L_{Rfi} \\
V_{fi}^{bd}\left(L_{Rfi};\delta_{Li}\right)=V_2^{bd}+V_3^{bd}+L_p\cdot\left[\displaystyle\int_{x_1^h}^{L_{tr1}}\tau^e\left(x^e\right)\cdot dx^e\right] \\
x_1^h=L_{tr}\left(\delta_{Li}\right)-L_{Rfi} \\
\delta_{Fi}\left(L_{Rfi};\delta_{Li}\right)=\delta^e\left(x_1^e\right)
\end{cases}
$$

$$
\begin{cases}
V_{fi}^{bd}\left(x_i^{tr}\right)=0 \quad \text{for} \quad 0\le x_i^{tr}\le x_2^{fs} \\
x_2^{fs}=L_{tr}\left(\delta_{Li}\right)-\left(L_{tr1}+L_{tr2}+L_{tr3}\right) \\
V_{fi}^{bd}\left(x_i^{tr}\right)=L_p\cdot\displaystyle\int_{L_{tr}\left(\delta_{Li}\right)-\left(L_{tr1}+L_{tr2}+x_i^{tr}\right)}^{L_{tr3}}\tau^{sf}\left(x^{sf}\right)\cdot dx^{sf} \quad \text{for} \quad x_2^{fs}<x_i^{tr}\le\left(x_2^{fs}+L_{tr3}\right) \\
V_{fi}^{bd}\left(x_i^{tr}\right)=L_p\cdot\left[\displaystyle\int_{L_{tr}\left(\delta_{Li}\right)-\left(L_{tr1}+x_i^{tr}\right)}^{L_{tr2}}\tau^{s}\left(x^{s}\right)\cdot dx^{s}+\int_0^{L_{tr3}}\tau^{sf}\left(x^{sf}\right)\cdot dx^{sf}\right]\ldots. \\
\ldots. \quad \text{for} \quad \left(x_2^{fs}+L_{tr3}\right)<x_i^{tr}\le\left(x_2^{fs}+L_{tr2}+L_{tr3}\right) \\
V_{fi}^{bd}\left(x_i^{tr}\right)=L_p\cdot\left[\displaystyle\int_{L_{tr}\left(\delta_{Li}\right)-x_i^{tr}}^{L_{tr1}}\tau^{e}\left(x^{e}\right)\cdot dx^{e}+\int_0^{L_{tr2}}\tau^{s}\left(x^{s}\right)\cdot dx^{s}+\int_0^{L_{tr3}}\tau^{sf}\left(x^{sf}\right)\cdot dx^{sf}\right]\ldots \\
\ldots. \quad \text{for} \quad \left(x_2^{fs}+L_{tr2}+L_{tr3}\right)<x_i^{tr}\le L_{tr,i}\left(L_{Rfi};\delta_{Li}\right)
\end{cases}
\tag{6.11}
$$

If $L_{Rfi}<L_{tr}\left(\delta_{Li}\right)$ and $L_{tr1}\le L_{tr}\left(\delta_{Li}\right)-L_{Rfi}\le\left(L_{tr1}+L_{tr2}\right)$, it is (case *d* in Fig. 6.5):

$$
\begin{cases}
L_{tr,i}\left(L_{Rfi};\delta_{Li}\right)=L_{Rfi} \\
V_{fi}^{bd}\left(L_{Rfi};\delta_{Li}\right)=V_3^{bd}+L_p\cdot\left[\int_{x_1^s}^{L_{tr}2}\tau^s\left(x^s\right)\cdot dx^s\right] \\
x_1^s=L_{tr}\left(\delta_{Li}\right)-\left(L_{Rfi}+L_{tr1}\right) \\
\delta_{Fi}\left(L_{Rfi};\delta_{Li}\right)=\delta^s\left(x_1^s\right)
\end{cases}
$$

$$
\begin{cases}
V_{fi}^{bd}\left(x_i^{tr}\right)=0 \quad \text{for} \quad 0\le x_i^{tr}\le x_2^{fs} \quad \text{with} \quad x_2^{fs}=L_{tr}\left(\delta_{Li}\right)-\left(L_{tr1}+L_{tr2}+L_{tr3}\right) \\
V_{fi}^{bd}\left(x_i^{tr}\right)=L_p\cdot\int_{L_{tr}\left(\delta_{Li}\right)-\left(L_{tr1}+L_{tr2}+x_i^{tr}\right)}^{L_{tr}3}\tau^{sf}\left(x^{sf}\right)\cdot dx^{sf} \quad \text{for} \quad x_2^{fs}<x_i^{tr}\le\left(x_2^{fs}+L_{tr3}\right) \\
V_{fi}^{bd}\left(x_i^{tr}\right)=L_p\cdot\left[\int_{L_{tr}\left(\delta_{Li}\right)-\left(L_{tr1}+x_i^{tr}\right)}^{L_{tr}2}\tau^s\left(x^s\right)\cdot dx^s+\int_0^{L_{tr}3}\tau^{sf}\left(x^{sf}\right)\cdot dx^{sf}\right] \quad .... \\
.... \quad \text{for} \quad \left(x_2^{fs}+L_{tr3}\right)<x_i^{tr}\le L_{tr,i}\left(L_{Rfi};\delta_{Li}\right)
\end{cases}
\tag{6.12}
$$

If $L_{Rfi}<L_{tr}\left(\delta_{Li}\right)$ and $\left(L_{tr1}+L_{tr2}\right)<L_{tr}\left(\delta_{Li}\right)-L_{Rfi}\le\left(L_{tr1}+L_{tr2}+L_{tr3}\right)$, it is (case *e* in Fig. 5.5):

$$
\begin{cases}
L_{tr,i}\left(L_{Rfi};\delta_{Li}\right)=L_{Rfi} \\
V_{fi}^{bd}\left(L_{Rfi};\delta_{Li}\right)=L_p\cdot\int_{x_1^{sf}}^{x_2^{L_{tr}3}}\tau^{sf}\left(x^{sf}\right)\cdot dx^{sf} \\
x_1^{sf}=L_{tr}\left(\delta_{Li}\right)-\left(L_{tr1}+L_{tr2}+L_{Rfi}\right) \\
\delta_{Fi}\left(L_{Rfi};\delta_{Li}\right)=\delta^{sf}\left(x_1^{sf}\right)
\end{cases}
$$

$$
\begin{cases}
V_{fi}^{bd}\left(x_i^{tr}\right)=0 \quad \text{for} \quad 0\le x_i^{tr}\le x_2^{fs} \quad \text{with} \quad x_2^{fs}=L_{tr}\left(\delta_{Li}\right)-\left(L_{tr1}+L_{tr2}+L_{tr3}\right) \\
V_{fi}^{bd}\left(x_i^{tr}\right)=L_p\cdot\int_{L_{tr}\left(\delta_{Li}\right)-\left(L_{tr1}+L_{tr2}+x_i^{tr}\right)}^{L_{tr}3}\tau^{sf}\left(x^{sf}\right)\cdot dx^{sf} \quad \text{for} \quad x_2^{fs}<x_i^{tr}\le L_{tr,i}\left(L_{Rfi};\delta_{Li}\right)
\end{cases}
\tag{6.13}
$$

If $L_{Rfi}<L_{tr}\left(\delta_{Li}\right)$ and $L_{tr}\left(\delta_{Li}\right)-L_{Rfi}>\left(L_{tr1}+L_{tr2}+L_{tr3}\right)$, it is (case *f* in Fig. 5.5):

$$\begin{cases} L_{tr,i}\left(L_{Rfi};\delta_{Li}\right)=L_{Rfi} \\ V_{fi}^{bd}\left(L_{Rfi};\delta_{Li}\right)=0 \\ x_1^{fs}=L_{tr}\left(\delta_{Li}\right)-\left(L_{tr1}+L_{tr2}+L_{tr3}+L_{Rfi}\right) \\ \delta_{Fi}\left(L_{Rfi};\delta_{Li}\right)=\delta^{fs}\left(x_1^{fs}\right) \\ V_{fi}^{bd}\left(x_i^{tr}\right)=0 \quad \text{for} \quad 0\le x_i^{tr}\le L_{tr,i}\left(L_{Rfi};\delta_{Li}\right) \end{cases} \tag{6.14}$$

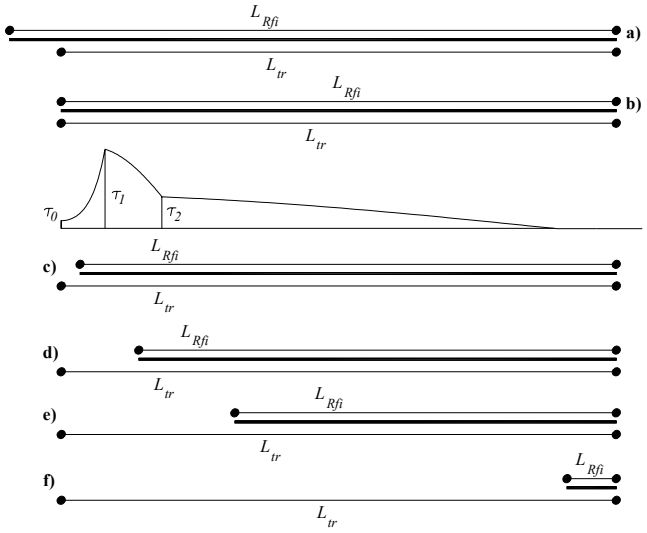

Fig. 6.5 – Possible configurations of bond stress with respect to finite resisting bond length and relative transfer length for an imposed slip $\delta_{Li} > \delta_3$.

7 Appraisal of the Model

The modeling strategy outlined above was appraised on the basis of the experimental results of the pull-out bending tests carried out by Sena-Cruz and Barros (2004). In that experimental program, those authors intentionally employed fiber reinforced concrete to avoid concrete fracture and force debonding to occur. Comparisons between the analytical and experimental results for the specimens tested in that occasion are plotted in Figs. 7.1 to 7.3. The generic label adopted in that occasion for each series, composed by three specimens, was BW_fcmXX_LbYY where W is the ordinal number of the specimen composing that series, XX is the concrete compression strength in MPa and YY is the resisting bond length in mm. The comparison regards both the relationship between force and imposed slip and force versus free end slip. From those comparisons a satisfactory data-fitting performance of the proposed model arises. The assumed values of the parameters entering the adopted bond stress-slip relationship were (Table 7.1): τ_0 equal to 3.0 MPa, τ_1 ranging from 16.5 to 25.0 MPa, τ_2 from 7.5 to 11.5 MPa, δ_1 from 0.06 to 0.20 mm, δ_2 from 0.50 to 1.40 mm and δ_3 from 13.0 to 19.0 mm. The variation of those parameters is due to the inevitable disturbance affecting the experimental results and attributable, for the cases herein examined, to the dissymmetry of the position of the strip cross section with respect to the groove's and/or some irregularities in the adhesive layer or on either the concrete surface or the composite surface.

Table 7.1 – Values for the bond parameters regarding the specimens tested by Sena and Barros (2004).

specimen	f_{cm} MPa	τ_0 MPa	τ_1 MPa	τ_2 MPa	δ_1 mm	δ_2 mm	δ_3 mm	L_{Rfi} mm
fcm35_Lb40	35.0	3.0	19.5	9.0	0.06	0.85	15.0	40.0
fcm35_Lb60	35.0	3.0	21.0	8.0	0.06	0.75	18.0	60.0
fcm35_Lb80	35.0	3.0	21.5	9.0	0.06	0.50	19.0	80.0
fcm45_Lb40	45.0	3.0	21.0	11.5	0.06	0.80	15.0	40.0
fcm45_Lb60	45.0	3.0	18.0	7.5	0.06	0.90	13.0	60.0
fcm45_Lb80	45.0	3.0	25.0	8.5	0.20	0.60	13.0	80.0
fcm70_Lb40	70.0	3.0	19.50	9.5	0.06	1.40	13.0	40.0
fcm70_Lb60	70.0	3.0	16.50	8.5	0.06	0.90	13.0	60.0
fcm70_Lb80	70.0	3.0	19.50	10.0	0.06	0.70	13.0	80.0

For all of the specimens, the FRP strip's section was 1.4 mm thick and 10.0 mm wide. The FRP's Young's Modulus was 166.6 GPa and the concrete cross section was 150 mm thick and 150 mm wide.

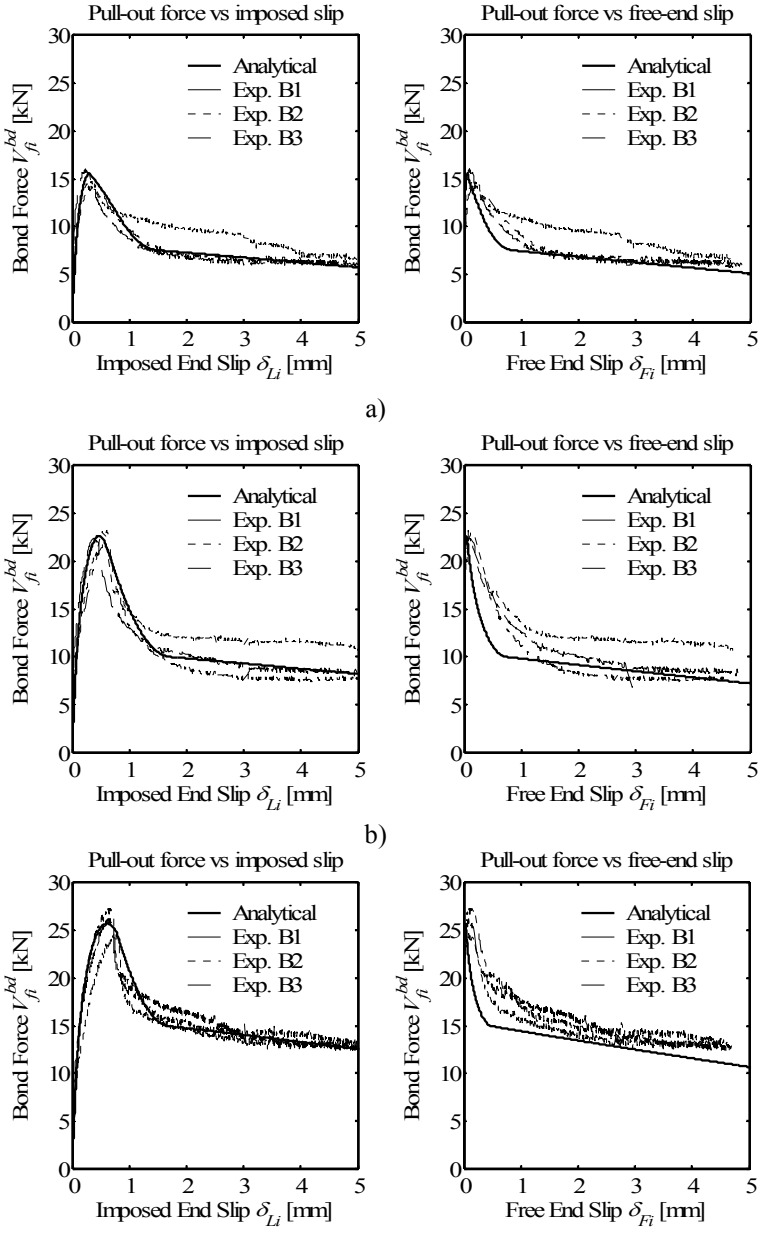

Fig. 7.1 – Appraisal of the proposed model for the pull-out tests by Sena-Cruz and Barros (2004) for specimens: fcm35_Lb40 a), fcm35_Lb60 b) and fcm35_Lb80 c).

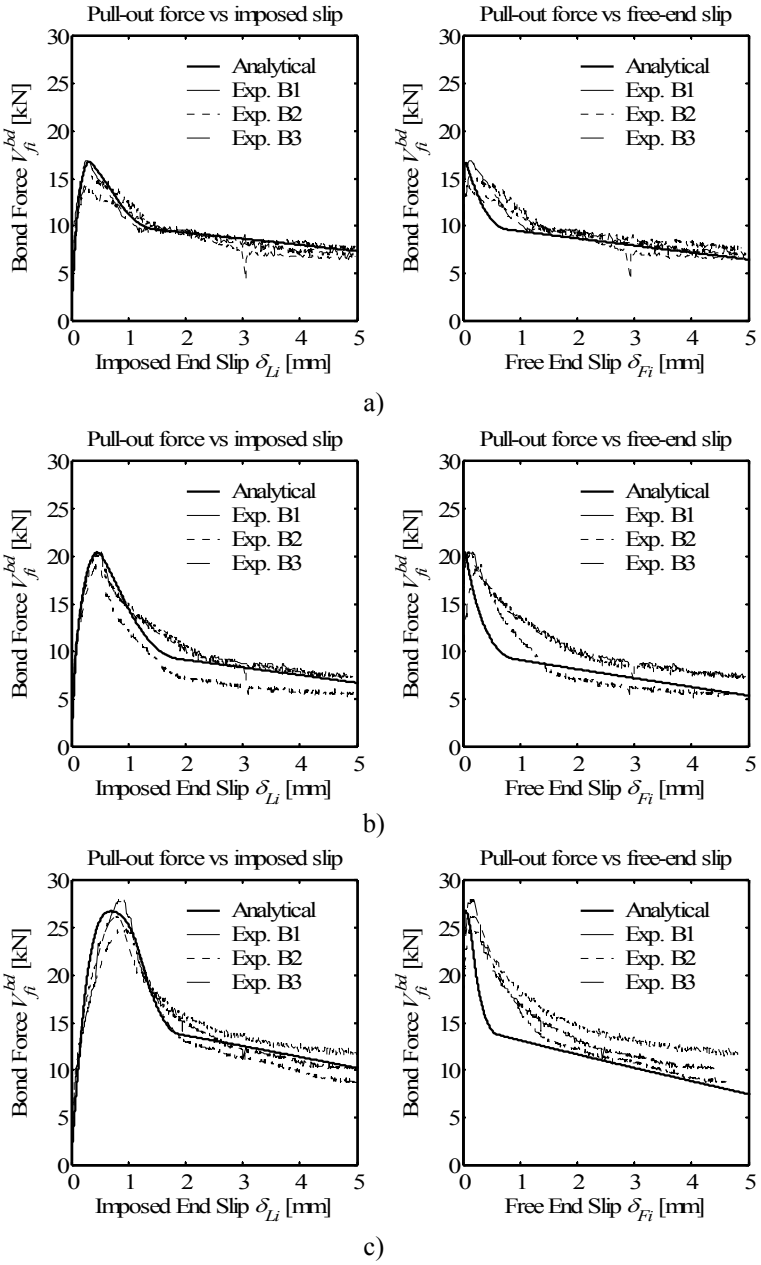

Fig. 7.2 – Appraisal of the proposed model for the pull-out tests by Sena-Cruz and Barros (2004) for specimens: fcm45_Lb40 a), fcm45_Lb60 b) and fcm45_Lb80 c).

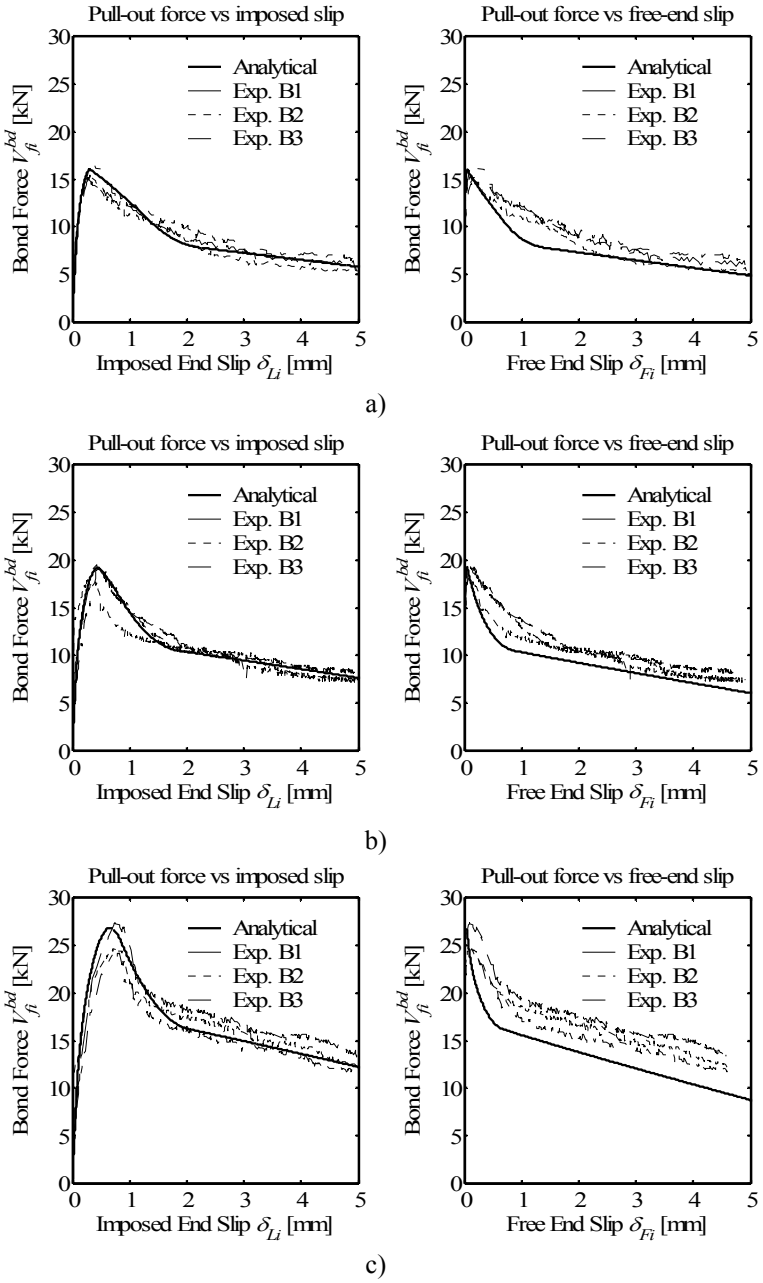

Fig. 7.3 – Appraisal of the proposed model for the pull-out tests by Sena-Cruz and Barros (2004) for specimens: fcm70_Lb40 a), fcm70_Lb60 b) and fcm70_Lb80 c).

8 Parametric analyses

A parametric study was carried out to evaluate the influence on the maximum force transmissible by bond V_{fi}^{bd} for the following values of the involved parameters (see Table 8.1): L_{Rfi} ranging from 40 to 1000 mm, a_f from 1.4 to 5.4 mm, b_f from 10 to 30 mm, E_f from 150 to 250 GPa, f_{cm} from 20 to 70 MPa, τ_0 from 0.5 to 5.0 MPa, τ_1 from 9 to 30 MPa, δ_1 from 0.05 to 0.75 mm. The results are show in Figs. 8.1 and 8.2. From those analyses it arises that higher Young's Modulus of either FRPs or concrete yield a negligible increase of peak load transmissible by bond (Fig. 8.1a-b). The increase of peak load is more significant for increased dimensions of the strip cross section (Fig. 8.1c-d), mainly the height of the strip. The peak load increases by increasing the resisting bond length up to a certain value beyond which any further increase does not produce any further gain in terms of resistance (Fig. 8.2a). That threshold value of length, according to the terminology already adopted for EBR, can be labelled as "effective bond length". In the same Fig. 8.2a, the values of the maximum force transferable due to concrete fracture V_{fi}^{cf} and to tensile rupture of the strip V_{fi}^{tr} are also plotted. The term V_{fi}^{cf} was calculated assuming a value of 30° for the angle between the axis and the generatrices of the semi-conical shaped fracture surface. From that plot, it emerges that, it can happen that concrete fracture and tensile rupture of the strip can be the commanding failure modes and debonding term can be completely unimportant.

As regards more specifically the influence of the parameters characterizing the local bond stress slip relationship, it arises that the peak load slightly decreases by increasing the value of τ_0 (Fig. 8.2b). Peak force increases by increasing τ_1 and decreases by increasing the relevant slip δ_1 (Fig. 8.2c-d).

Table 8.1 – Values for the bond parameters regarding the specimens tested by Sena and Barros (2004).

study	a_f mm	b_f mm	a_c mm	b_c mm	E_f GPa	f_{cm} MPa	τ_0 MPa	τ_1 MPa	τ_2 MPa	δ_1 mm	δ_2 mm	δ_3 mm	L_{Rfi} mm
1	1.4	10.0	15.0	15.0	**150-250**	35.0	3.0	20.5	8.5	0.04	0.8	20.0	40.0
2	1.4	10.0	15.0	15.0	166.6	**20-70**	3.0	20.5	8.5	0.04	0.8	20.0	40.0
3	**1.4-5.4**	10.0	15.0	15.0	166.6	35.0	3.0	20.5	8.5	0.04	0.8	20.0	40.0
4	1.4	**10-30**	15.0	15.0	166.6	35.0	3.0	20.5	8.5	0.04	0.8	20.0	40.0
5*	1.4	10.0	15.0	15.0	166.6	35.0	3.0	20.5	8.5	0.04	0.8	20.0	**5-1000**
6	1.4	10.0	15.0	15.0	166.6	35.0	**0.5-5.0**	20.5	8.5	0.04	0.8	20.0	40.0
7	1.4	10.0	15.0	15.0	166.6	35.0	3.0	**9.0-30.0**	8.5	0.04	0.8	20.0	40.0
8	1.4	10.0	15.0	15.0	166.6	35.0	3.0	20.5	8.5	**0.05-0.75**	0.8	20.0	40.0

* for that case, the concrete fracture strength V_{fi}^{cf} was evaluated assuming $\alpha = 30°$ and the tensile rupture based term, V_{fi}^{tr} assuming strips' tensile strength of 3.774 GPa.

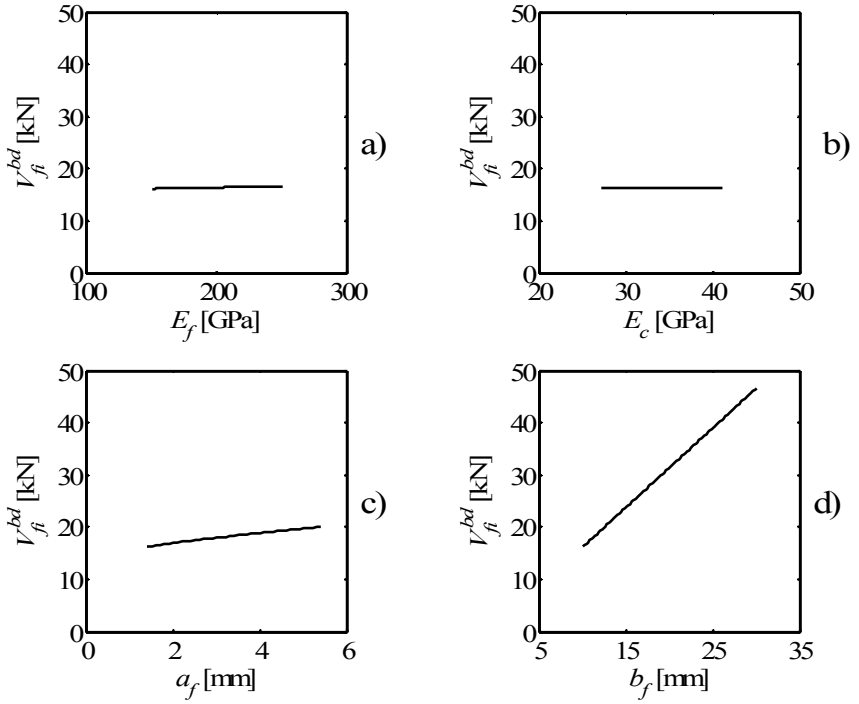

Fig. 8.1 – Parametric study: influence of the FRPs' Young's Modulus (a), concrete Young's Modulus (b), strips' thickness (c) and width (d) on the maximum value of the force transmissible by bond.

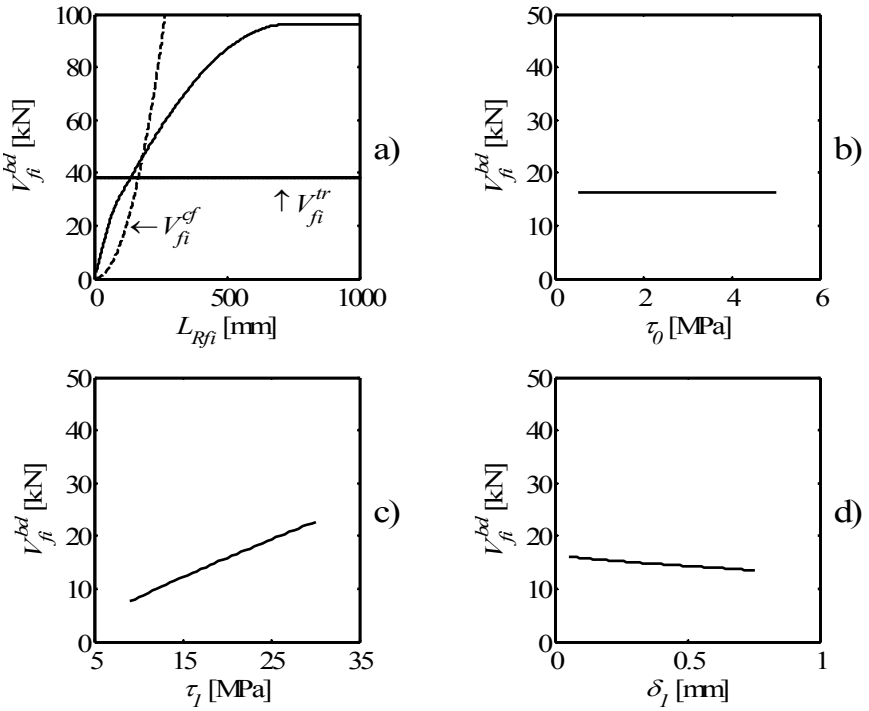

Fig. 8.2 – Parametric study: influence of strip resisting bond length (a), the parameter τ_0 (b), the parameter τ_1 (c) and δ_1 (d) on the maximum value of the force transmissible by bond.

9 Conclusions

The need to improve an already existing analytical model developed to predict the NSM FRP strips' shear strength contribution to RC beams, led to further address some issues related to debonding failure mode and the interaction between bond-based force transfer and concrete semi-conical tensile fracture. Due to the relative novelty of the employment of powerful adhesives in the ambit of structural engineering, the necessity arises to further investigate the micromechanical and chemical properties of the materials involved. A new physical-mechanical interpretation of debonding process and a corresponding simplified analytical model of the local bond stress-slip relationship were proposed. The entire debonding process was described and closed-form analytical expressions to be implemented in the model for shear were derived. The comparison between the analytical predictions and some of the most accredited experimental results available to date, showed the high level of accuracy of the proposed model. The influence of the main geometrical and mechanical parameters on the maximum value of the force transferred by bond was also investigated.

10 ACKNOWLEDGEMENTS

The authors of the present work wish to acknowledge the support provided by the "Empreiteiros Casais", S&P®, Secil (Unibetão, Braga) and Degussa® Portugal. The study reported in this paper forms a part of the research program "CUTINSHEAR - Performance assessment of an innovative structural FRP strengthening technique using an integrated system based on optical fiber sensors" supported by FCT, POCTI/ECM/59033/2004. This work has been partially carried out under the program "Dipartimento di Protezione Civile – Consorzio RELUIS", signed on 2005-07-11 (n. 540), Research Line 8, whose financial support is greatly appreciated.

11 References

Bianco, V., Barros, J.A.O., Monti, G., (2006). "Shear Strengthening of RC beams by means of NSM laminates: experimental evidence and predictive models", Technical report 06-DEC/E-18, Dep. Civil Eng., School Eng. University of Minho, Guimarães- Portugal.

Bianco, V., Barros, J.A.O., Monti, G., (2007a). "A new approach for modeling the NSM shear strengthening contribution in reinforced concrete beams", FRPRCS-8, University of Patrass, Greece,16-18 July, ID 8-13.

Bianco, V., Barros, J.A.O., Monti, G., (2007b). "Influence of the concrete mechanical properties on the efficacy of the shear strengthening intervention on RC beams by NSM technique", Asia-Pacific Conference on FRP in Structures, University of Hong Kong, China,12-14 December.

Bianco, V., Barros, J.A.O., Monti, G., (2007c). "Shear Strengthening of RC beams by means of NSM laminates: a proposal for modelling debonding", Technical report 06-DEC/E-18, Dep. Civil Eng., School Eng. University of Minho, Guimarães- Portugal.

Borchert, K., Zilch, K., (2007), "A general bond stress-slip relationship for NSM FRP strips", FRPRCS-8, University of Patrass, Greece,16-18 July, ID 8-1.

Cook, R.A., Kunz, J., Fuchs, W., Konz, R.C., (1998), "Behaviour and design of Single Adhesive Anchors under Tensile Load in Uncracked Concrete", ACI Structural journal, Vol. 95, No. 1, January/February, pp. 9-26.

De Lorenzis, L., Rizzo, A., (2006). "Behaviour and capacity of RC beams strengthened in shear with NSM FRP reinforcement", 2nd Int. fib Congress, Naples-Italy, June 5-8, Paper ID 10-9 in CD.

Dias, S.J.E., Barros, J.A.O., (2006). "NSM CFRP Laminates for the Shear Strengthening of T Section RC Beams", 2nd International fib Congress, Naples, Italy, ID 10-58.

Dias, S.J.E., Bianco, V., Barros, J.A.O., Monti, G., (2007). "Low strength concrete T cross section RC beams strengthened in shear by NSM technique", Workshop-Materiali ed Approcci Innovativi per il Progetto in Zona Sismica e la Mitigazione della Vulnerabilità delle Strutture, University of Salerno, Italy, 12-13 February.

Dias, S.J.E., Bianco, V., Barros, J.A.O., Monti, G., (2007). "Low strength concrete T cross section RC beams strengthened in shear by NSM technique", Workshop-Materiali ed Approcci Innovativi per il Progetto in Zona Sismica e la Mitigazione della Vulnerabilità delle Strutture, University of Salerno, Italy, 12-13 February.

Kreyszig, Erwin, (1998) "Advanced Engineering Mathematics", John Wiley and Sons, Inc. New York.

Monti, G., Liotta, M.A., (2006). "Tests and design equations for FRP-strengthening in shear", Construction and Building Materials,_____.

Mohammed Ali, M.S., Oehlers, D.J., Seracino, R. (2006). "Vertical shear interaction model between external FRP transverse plates and internal stirrups", Engineering Structures 28, 381-389.

Sekulic, A., Curnier, A., (2006). "An original epoxy-stamp on glass-disc specimen exhibiting stable debonding for identifying adhesive properties between glass and epoxy", International Journal of Adhesion and Adhesives, Vol. 27, pp. 611-620.

Sena-Cruz, J.M. (2004). "Strengthening of concrete structures with near-surface mounted CFRP laminate strips" PhD Thesis, Department of Civil Engineering, University of Minho, Guimarães- Portugal.

Sena-Cruz, J.M., Barros, J.A.O., (2004). "Bond between near-surface mounted CFRP laminate strips and concrete in structural strengthening", Journal of Composites for Construction, ASCE, Vol. 8, No. 6, pp. 519-527.

Yuan, H., Teng, J.G., Seracino, R., Wu, Z.S., Yao, J. (2004). "Full-range behavior of FRP-to-concrete bonded joints", Engineering Structures, 26, 553-565.

Zhai, L.L., Ling, G.P., Wang, Y.W., (2007). "Effect of nano-Al2O3 on adhesion strength of epoxy adhesive and steel", International Journal of Adhesion and Adhesives, doi:10.1016/j.ijadhadh.2007.03.05.